

Supporting Information for

Spectroscopic characterization and reactivity studies of a copper(II) iminoxyl radical complex

Simarjeet Kaur,^a Avijit Das,^a Lucia Velasco,^b Maxime Sauvan,^b Moumita Bera,^a Ashok Ugale,^b Asterios Charisiadis^b, Dooshaye Moonshiram,^{*b} Sayantan Paria^{*a}

^[a]Department of Chemistry, Indian Institute of Technology Delhi, Hauz Khas, New Delhi-110016; E-mail: sparia@chemistry.iitd.ac.in

^[b]Instituto de Ciencia de Materiales de Madrid, Consejo Superior de Investigaciones Científicas, Sor Juana Inés de la Cruz, 3, 28049 Madrid, Spain; Email: dooshaye.moonshiram@csic.es

Table of Contents

Table of Contents	S1
General and physical methods used in the study	S2–S9
Synthesis and Characterization	S9–S30
DFT Studies	S30–S46
References	S46

Author Contributions

SK synthesized and characterized the Cu complexes used in this study. AD and MB also contributed to the synthesis part. SK performs and analyses all kinetic studies. LV, MS, AU, and AC contributed to the preparation of the samples for X-ray absorption spectroscopy studies, data collection, analysis, and DFT studies. DM supervised the X-ray absorption spectroscopy and DFT studies described in the study. SP supervised the project. All authors contributed to writing the manuscript.

General. All chemicals used in this study were purchased from commercial sources and used as received. Anhydrous acetonitrile, and methanol were purchased from Sigma-Aldrich and used as received. $\text{Cu}(\text{ClO}_4)_2 \cdot 6\text{H}_2\text{O}$ and ferrocene substrates were procured from Sigma Aldrich and used without further purification. Diethyl ether was purified over sodium/benzophenone. The ligand H_2L_1 was prepared following a literature procedure.¹ TEMPOH was synthesized according to the literature procedure.² Synthesis and manipulations of all air-sensitive compounds were performed either in an N_2 -filled glovebox (Vigor Tech) or using standard Schlenk techniques. Caution: *Although no problems were encountered during the synthesis of the complex, perchlorate salts are potentially explosive and should be handled with care!*³

Experimental Section

Elemental analysis. A PerkinElmer 2400 Series II CHNS/O instrument was used to perform the CHN analysis of the Cu complexes used in this study.

Infrared Spectroscopy. Fourier transform infrared spectra of the Cu complexes (**1**, **1-ox**) were recorded on a KBr pellet in a Nicolet protégé 460 ESP instrument.

Mass spectra. ESI mass spectra of the ligands and Cu complexes were recorded in Waters Xevo-G2XQTOF instruments with the electrospray ionization (ESI) source. GC-mass spectra of the organic compounds were measured in an Agilent 7890B GC system fitted with an FID detector and an Agilent 5977B GC/MSD mass detector.

NMR spectroscopy. The ^1H -NMR spectra of the organic compounds and Cu complex were recorded in a Bruker 400 MHz (DPX-400) or 500 MHz (DPX-500) NMR instruments. Low-temperature NMR of the Cu complexes was measured in a JEOL-JNM-ECA Series (Delta V4.3)-400 MHz-FT-NMR instrument. Solution magnetic moments of the Cu complexes were determined by Evans' method following literature procedures.⁴

Electron Paramagnetic Resonance Spectroscopy. X-band EPR data described in this study were recorded in a Bruker A300 spectrometer at 77 K using a liquid N_2 finger Dewar. The EPR samples of **1** (2 mM) were prepared in MeOH. The samples (~400 μL) were introduced in the EPR tubes and sealed using septa inside an N_2 -filled glove box. Then, the data were recorded at 77 K. EPR data was processed using Bruker WinEPR and simulated using SymFonia software.

Preparation of 1-ox: A 400 μL methanol solution of **1** (2 mM) was introduced in an EPR tube inside the glove box and sealed with a septum. The EPR tube was taken outside the glove box and placed in an Eyla low-temperature reaction bath pre-cooled at $-40\text{ }^\circ\text{C}$. After 5 minutes, one equiv. of ceric ammonium nitrate (30 μL of a 40 mM methanol solution, one equiv.) was slowly introduced into the reaction solution using a Hamilton microliter syringe. Then, the solution was quickly purged with nitrogen for 2 minutes to make the solution homogeneous before dipping the tube in a liquid nitrogen bath. The sample was then taken for the EPR measurement.

Electrochemical Measurements. Cyclic voltammetry (CV) and differential pulse voltammetry (DPV) data reported in this study were recorded using a CH Instrument (CHI 760E, CH Instrument, USA) in a typical three-electrode set-up. A glassy carbon working

electrode, Pt wire counter electrode, and Ag/AgCl in saturated KCl or Ag wire as pseudo reference electrodes were utilized during the measurements. All measurements were made in methanol or acetonitrile solutions at 25 °C using ferrocene (Fc) as the internal standard (with respect to the Fc⁺/Fc couple) and tetrabutylammonium perchlorate (ⁿBu₄NClO₄) as the supporting electrolyte. The $E_{1/2}$ values for the ferrocene derivatives were calculated from the DPV data using the Parry-Osteryoung Equation ($E_{1/2} = E_p + \Delta E/2$).⁵ ΔE is the amplitude.

Kinetic Study. All of the kinetic measurements reported in this study were conducted in an Agilent 8454 Diode Array Spectrophotometer equipped with a liquid nitrogen-controlled UNISOKU low-temperature cryostat, which can control the temperature of a reaction solution over a temperature range of -80 to 100 °C within ± 0.1 °C accuracy.

A 10 or 25 mL stock solution of the Cu(II) complexes (**1**, 0.1–0.3 mM) in methanol was prepared inside a glove box. A 2.4 mL solution of the complex solution was introduced in a long-neck cuvette inside the glove box, sealed with a rubber septum, and taken outside the glove box. The cuvette was subsequently placed in the pre-cooled cryostat fitted at the spectrophotometer at a desired temperature. Then, a methanolic solution of ceric ammonium nitrate (one equiv. with respect to complex) was introduced into the Cu(II) complex solution at -40 °C to -60 °C via a Hamilton syringe connected to a long needle. Once the formation of the oxidized Cu(II) complex was complete (**1-ox**), a substrate solution (10–100 μ L) was added to the reaction mixture, stirred vigorously, and the reaction was monitored by UV-vis spectroscopy following the decay of species **1-ox**. Pseudo-first-order rate-constant (k_{obs}) was estimated from the slope of a plot of $\ln(A-A_\infty)$ vs. time (s), and second-order rate-constant (k_2) was determined from the slope of a plot of k_{obs} vs [substrate]. In the reactions studied under second-order reaction conditions, k_2 values were determined from the slope of a plot of $1/[\mathbf{1-ox}]$ vs. time (s).

X-ray Crystallography. Single crystals of **1** suitable for single-crystal X-ray diffraction studies were selected from an acetonitrile/diethyl ether solution containing the crystals and immediately immersed into the Paratone oil, followed by mounting on a nylon loop under a 100 K nitrogen cold stream. Data collections were performed on a Bruker D8 VENTURE Microfocus diffractometer equipped with PHOTON II Detector, with Mo K α radiation ($\lambda = 0.71073$ Å), controlled by the APEX III (v2017.3-0) software package. The raw data were integrated and corrected for Lorentz and polarization effects with the aid of the Bruker APEX III program suite.⁶ Structures were solved by the intrinsic phasing method and refined against all data in the reported 2θ ranges by full-matrix least squares method based on F2 using the SHELXL program suite.⁷ Hydrogen atoms at idealized positions were incorporated in final refinements. The non-hydrogen atoms were treated anisotropically. Diagrams for the complexes were prepared using the Mercury software.⁸ The crystallographic data and final agreement factors for the complex are provided in Table S1, S2.

Table S1. Summary of X-ray crystallographic data of Cu complex **1**.

	1
Empirical formula	C ₂₂ H ₂₁ ClCuN ₆ O ₆
Formula weight	564.45
Crystal system	Monoclinic
Space group	P 21/n
<i>a</i> (Å)	10.905(6)
<i>b</i> (Å)	19.645(10)
<i>c</i> (Å)	11.608(6)
α (deg.)	90
β (deg.)	104.342(17)
γ (deg.)	90
Volume (Å ³)	2409(2)
<i>Z</i>	4
<i>D</i> _{calcd.} (mg/m ³)	1.556
μ Mo-K α (mm ⁻¹)	1.069
<i>F</i> (000)	1158.8
θ range (deg.)	2.09 to 32.840
Reflections collected	56315
Reflections unique	4101
<i>R</i> (int)	0.0842
Data (<i>I</i> > 2 σ (<i>I</i>))	8050
Parameters refined	332
Goodness-of-fit on <i>F</i> ²	1.138
<i>R</i> 1 [<i>I</i> > 2 σ (<i>I</i>)]	0.0846
<i>wR</i> 2	0.2198

Table S2. Important bond lengths (Å) and bond angles (°) for complex **1**.

Bond Length (Å)	1
Cu(1)–N(1)	1.912(3)
Cu(1)–N(2)	1.929(4)
Cu(1)–N(3)	1.920(4)
Cu(1)–N(4)	1.916(3)
Cu(1)–O(3)	2.419(4)
N(1)–N(2)	2.892(6)
O(1)–O(2)	2.515(6)
Bond angle (°)	
N(1)–Cu(1)–N(2)	97.7(2)
N(2)–Cu(1)–N(3)	174.0(2)
N(3)–Cu(1)–N(4)	94.2(1)
N(1)–Cu(1)–N(3)	83.8(2)
N(2)–Cu(1)–N(4)	83.6(2)
N(1)–Cu(1)–N(4)	173.4(2)

X-ray Absorption Spectroscopy (XAS) Methods. X-ray absorption spectra were collected at the Diamond light Source (Oxford, UK) on bending magnet beamline BL18 at electron energy 8.98 KeV and an average current of 100 mA. The radiation was monochromatized by Si(110) crystal monochromator. The intensity of the X-rays were monitored by three ion chambers (I_0 , I_1 and I_2) filled with 70 % nitrogen and 30 % Helium and placed before the sample (I_0) and after the sample (I_1 and I_2). Cu metal was placed between ion chambers I_1 and I_2 , and its absorption was recorded with each scan for energy calibration. Cu XAS energy was calibrated by the first maxima in the second derivative of the copper's metal foil's X-ray absorption near edge structure (XANES) spectrum. The samples were kept at 20 K in a He atmosphere at ambient pressure and recorded as fluorescence excitation spectra using a 44-element energy-resolving Ge detector. The solution complexes were measured in the continuous helium flow cryostat in fluorescence mode. Around 40 XAS spectra of each sample were collected. Care was taken to measure at several sample positions on each sample, and no more than 5 scans were taken at each sample position. In order to reduce the risk of sample damage by x-ray radiation, 80% flux was used (beam size 1000 μm (Horizontal) x 2000 μm (Vertical)), and no damage was observed scan after scan to any samples. All samples were also protected from the X-ray beam during spectrometer movements by a shutter synchronized with the scan program.

Cu XAS energy was calibrated by the first maxima in the second derivative of the copper's metal X-ray Absorption Near Edge Structure (XANES) spectrum.

Extended X-ray Absorption Fine Structure (EXAFS) Analysis. Athena software⁹ was used for data processing. The energy scale for each scan was normalized using the copper metal standard. Data in energy space were pre-edge corrected, normalized, deglitched (if necessary), and background corrected. The processed data were next converted to the photoelectron wave vector (k) space and weighted by k^2 . The electron wave number is defined as $k = [2m(E - E_0)/\hbar^2]^{1/2}$, E_0 is the energy origin or the threshold energy. K-space data were truncated near the zero crossings $k = 1.5$ to 14 \AA^{-1} in Cu EXAFS before Fourier transformation. The k-space data were transferred into the Artemis Software for curve fitting. In order to fit the data, the Fourier peaks were isolated separately, grouped together, or the entire (unfiltered) spectrum was used. The individual Fourier peaks were isolated by applying a Hanning window to the first and last 15% of the chosen range, leaving the middle 70% untouched. Curve fitting was performed using *ab initio*-calculated phases and amplitudes from the FEFF8¹⁰ program from the University of Washington. *Ab initio*-calculated phases and amplitudes were used in the EXAFS equation S1.

$$\chi(k) = S_0^2 \sum_j \frac{N_j}{kR_j^2} f_{\text{eff}_j}(\pi, k, R_j) e^{-2\sigma_j^2 k^2} e^{\frac{-2R_j}{\lambda_j(k)}} \sin(2kR_j + \phi_j(k)) \quad (\text{S1})$$

where N_j is the number of atoms in the j^{th} shell; R_j the mean distance between the absorbing atom and the atoms in the j^{th} shell; $f_{\text{eff}_j}(\pi, k, R_j)$ is the *ab initio* amplitude function for shell j , and the Debye-Waller term $e^{-2\sigma_j^2 k^2}$ accounts for damping due to static and thermal disorder in absorber-backscatterer distances. The mean free path term $e^{\frac{-2R_j}{\lambda_j(k)}}$ reflects losses due to inelastic scattering, where $\lambda_j(k)$, is the electron mean free path. The oscillations in the EXAFS spectrum are reflected in the sinusoidal term $\sin(2kR_j + \phi_j(k))$, where $\phi_j(k)$ is the *ab initio* phase function for shell j . This sinusoidal term shows the direct relation between the frequency of the EXAFS oscillations in k-space and the absorber-backscatterer distance. S_0^2 is an amplitude reduction factor.

The EXAFS equation¹¹ (Eq. S1) was used to fit the experimental Fourier isolated data (q-space) as well as unfiltered data (k-space) and Fourier transformed data (R-space) using N , S_0^2 , E_0 , R , and σ^2 as variable parameters. N refers to the number of coordination atoms surrounding Cu for each shell. The quality of fit was evaluated by R-factor (Eq. S2) and the reduced Chi² value. The deviation in E_0 ought to be less than or equal to 10 eV. R-factor less than 2 % denotes that the fit is good enough¹¹ whereas R-factor between 2 and 5 % denotes that the fit is correct within a consistently broad model. The reduced Chi² value is used to compare fits as more absorber-backscatter shells are included to fit the data. A smaller reduced Chi² value implies a better fit. Similar results were obtained from fits done in k , q , and R -spaces.

$$R - factor = \frac{\sum_i(\text{difference between data and fit}_i)^2}{\sum_i(\text{data})^2} \quad (\text{S2})$$

The pre-edge area fits were carried out with an error function and a Gaussian function in the Athena¹¹ software using the peak-fitting function. The formulas for the error(erf) and Gaussian function employed for the pre-edge fits are shown in equations S3 and S4.

Error function:

$$A \left[\text{erf} \left(\frac{e - E_0}{w} \right) + 1 \right] \quad (\text{S3})$$

Gaussian function:

$$\left(\frac{A}{w\sqrt{2\pi}} \right) \exp \left[-\frac{(e - E_0)^2}{(2w^2)} \right] \quad (\text{S4})$$

Where A corresponds to the amplitude; w, the width; E_0 , the centroid of the pre-edge and near edge peaks and e, the x-ray energy.

The parameters E_0 , A and w used for each sets of functions are tabulated below (Table S5).

DFT Calculations. The DFT optimization calculations were performed using the ORCA (Version 5.0.4) program package developed by Neese¹² and co-workers. The geometry optimizations were carried out using the solid-state (XRD) as a starting point. The calculations were carried out using the BP86 exchange-correlation functional¹³ in combination with the triple zeta valance polarization functions (def2-TZVP),¹⁴ the continuum-like polarizable model (CPCM) model with acetonitrile as a solvent, and the atom-pairwise dispersion correction with the Becke-Johnson damping scheme (D3BJ).¹⁵

The RI¹⁶ approximation were used to accelerate Coulomb and exchange integrals for the ground and excited state calculations respectively. The default GRID settings were further used for the self-consistent field iterations and for the final energy evaluation. The calculated structures were confirmed to be minima based on a check of the energies and the absence of imaginary frequencies from frequency calculations carried out on the optimized geometries. DFT calculations of both the initial and oxidized form of the Cu complex are shown in Table S4 and Appendix. In order to calculate the electron density differences between **1** and **1-ox**, the optimized geometry and parameters of **1** were used to perform a single-point energy calculation on **1-ox**. The total electron densities of **1** and **1-ox** were subsequently attained through Multiwfn: A Multifunctional Wavefunction Analyzer program package developed by

Lu and co-workers¹ and subtracted and visualized from one another with the Chemcraft software (Table S7).

Time-dependent (TD)-DFT XANES Calculations. Time-dependent DFT (TD)-DFT calculations for the optical and XANES spectra of the Cu complexes were carried out using the hybrid-DFT functional B3LYP. The TD-DFT XANES simulations were in this case performed with the B3LYP¹⁷ as functional with the def2-TZVP triple-zeta¹⁷ basis sets together with the D3BJ dispersion correction effects with dense integration grids and the CPCM model. The def2-TZVP/J auxiliary basis set was also employed. A broadening of 3 eV was applied to all XANES calculated spectra and shifted by +194.5 eV relative to experimental spectra. Up to 50 and 150 roots were calculated for the optical and XANES spectra, respectively.

Table S3. EXAFS Fits parameters.

Sample	Fit	Reg ion	Shell,N	R, Å	E ₀	ss. ² (10 ⁻³)	R-factor	Reduced Chi-square
1	1	I	Cu-N,4	1.94	2.8	3.4	0.0054	345
	2	I,II	Cu-N, 4 Cu-C/O, 8 Cu-C, 12	1.95 2.87 3.11	5.0	3.4 16 1.9	0.0061	189
3		I,II	Cu-N, 4	1.94	3.6	3.5	0.0043	184
			Cu/O, 1	2.35		9.4		
			Cu-C/O, 8	2.86		19		
			Cu-C, 12	3.11		1.9		
1-ox	4	I	Cu-N,5	1.95	2.7	5.5	0.0157	953
	5	I,II	Cu-N, 4	1.96	3.6	4.5	0.0774	1277
			Cu/O, 1	2.31		4.9		
			Cu-C/O, 8	2.82		8.4		
			Cu-C, 12	3.16		3.3		
	6	I,II	Cu-N, 5 Cu-C/O, 8 Cu-C, 12	1.96 2.86 3.09	5.0	5.8 14 1.2	0.0157	467

* The amplitude reduction factor S0² was fixed to 1. Region I refers to the EXAFS spectra region between apparent distances 1.2 -2 Å, Regions I ,II refer to that between 1.2-3 Å. We note that the data resolution, the ability to distinguish between 2 bond distances, given by $\pi/2\Delta k$ is ~ 0.126 Å.

Table S4. Summary of the bond distances of **1** and **1-ox**, derived from EXAFS, XRD, and DFT analysis Bond distances are in Å.

Complexes	EXAFS (Å)	XRD (Å)	DFT (Å)
1	Cu-N (4): 1.94 Cu-O(1):	Cu-N: 1.91982, 1.91215, 1.92887,	Cu-N: 1.93181, 1.95127, 1.95686, 1.94610 Cu-N_{avg} = 1.947

	2.35	Cu-N_{avg} = 1.919 Cu-O (Perchlorate) = 2.41869	Cu-O (Perchlorate) = 2.44430
1-ox	Cu-N (5): 1.96		Cu-N: 1.96855, 1.97209, 1.98871, 1.98035 Cu-N (bound acetonitrile) = 2.06838 Cu-N_{avg} = 1.996

Table S5. Pre-edge parameter fits for **1** and **1-ox**.

1			
Function	Centroid	Amplitude	Width
Erf	8983.5	0.090	3.2
Gauss	8979.4	0.105	1.8
Pre-edge area	10.5 units		
1-ox			
Function	Centroid	Amplitude	Width
Erf	8984.04	0.090	3.2
Gauss	8979.4	0.100	1.8
Pre-edge area	10.0 units		

The pre-edge area peaks fitting were further re-carried out in the Fityk¹⁸ software and as previously demonstrated¹⁹, and the same pre-edge peak areas of 10.5, and 10.0 units were obtained for **1**, and **1-ox**, respectively, thus confirming the fit procedure employed in the Athena⁹ software.

Synthesis

H₂L₁-d₅ was synthesized as described in Scheme S1, and similar experimental conditions were followed as described for the preparation of H₂L₁.¹ Nitrobenzene-d₅ was synthesized from benzene-d₆ by using HNO₃/H₂SO₄ as the oxidant according to the literature procedure.²⁰ Aniline-d₅ was further synthesized by reducing nitrobenzene-d₅ by Sn/HCl using the same procedure as for the reduction of natural nitrobenzene.

6-(2-methyl-1,3-dioxolan-2-yl)-N-(6-(2-methyl-1,3-dioxolan-2-yl)pyridin-2-yl)-N-(phenyl-d₅)pyridin-2-amine (P3): Yield: 83 % (1.45 g). ¹H NMR (CDCl₃, 500MHz): δ 1.6 (s, 6H, CH₃), 3.88 (m, 4H, CH₂), 3.99 (m, 4H, CH₂), 7.01 (d, 2H, ArH), 7.11 (d, 2H, ArH), 7.51 (t, 2H, ArH). ¹³C NMR (CDCl₃, 100MHz): δ 24.46, 65.19, 108.6, 113, 115.7, 137.5, 157.3, 158.9. ESI-MS [C₂₄H₂₀D₅N₃O₄ + H⁺]: 425.2232 (calculated), 425.2215 (observed). IR (KBr, cm⁻¹): 3440 (br), 2986 (s), 2882 (s), 2933 (s), 1571 (s), 1440 (s), 1323 (s), 1196 (s), 1036 (s), 950 (s), 876 (s), 803 (s), 742 (s), 566 (m).

1,1'-(((phenyl-d₅)azanediy)bis(pyridine-6,2-diyl))bis(ethan-1-one) (P4): Yield: 90% (1.06 g). ¹H NMR (CDCl₃, 500MHz): δ 2.4 (s, 6H, CH₃), 7.31 (d, 2H, ArH), 7.68-7.33 (m, 4H, ArH).

^{13}C NMR (CDCl_3 , 100MHz): δ 25.57, 115.6, 119.7, 137.92, 151.69, 156.69, 200.19. ESI-MS [$\text{C}_{20}\text{H}_{12}\text{D}_5\text{N}_3\text{O}_2 + \text{Na}^+$]: 359.1527 (calculated), 359.1523 (observed). IR (KBr, cm^{-1}): 3434 (br), 2925 (m), 2885 (br), 1690 (s), 1575 (s), 1439 (s), 1331 (m), 1250 (s), 1159 (s), 1156 (s), 954 (s), 805 (s), 728 (s), 593 (s), 551 (m).

(1E,1'E)-1,1'-(((phenyl-d5)azanediyl)bis(pyridine-6,2-diyl))bis(ethan-1-one) dioxime (H_2L_1-d_5): Yield: 77% (0.82 g). ^1H NMR (dmso- d_6 , 500MHz): δ 1.9 (s, 6H, CH_3), 6.96 (d, 2H, ArH), 7.46 (d, 2H, ArH), 7.67 (t, 2H, ArH), 11.42 (s, 2H, NOH). ^{13}C NMR (dmso- d_6 , 100MHz): δ 10.54, 114.1, 115.98, 138.47, 153.19, 154.74, 156.77. ESI-MS [$\text{C}_{20}\text{H}_{14}\text{D}_5\text{N}_5\text{O}_2 + \text{H}^+$]: 367.1926 (calculated), 367.1918 (observed). IR (KBr, cm^{-1}): 3233(br), 2922 (m), 1739 (br), 1566 (s), 1446 (s), 1363 (m), 1296 (m), 1158 (s), 1014 (s), 921 (s), 800 (s), 728 (s), 679 (m), 550 (m).

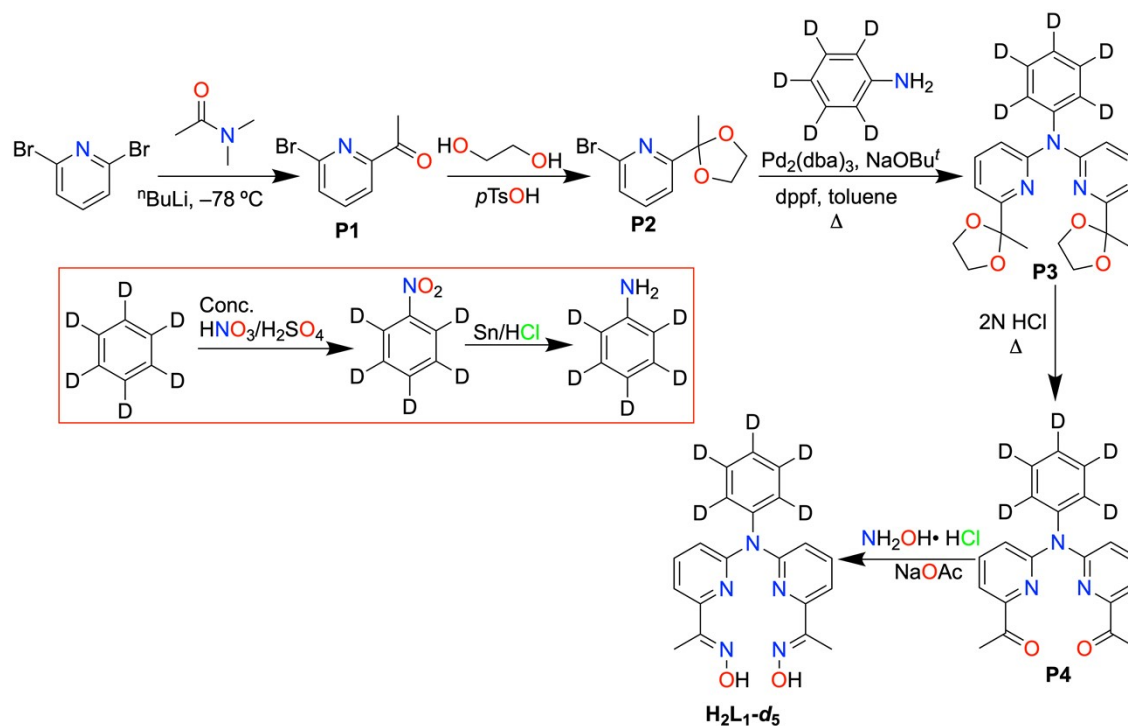
N^1 , N^3 -bis(2-acetylphenyl)-2,2-diethylmalonamide (P5): 1-(2-aminophenyl)ethan-1-one (1g, 7.4 mmol) was dissolved in dry diethyl ether, and the solution was stirred at 0 °C in ice bath. Then 2,2-diethylmalonyl dichloride (728.9 mg, 3.7 mmol) was added dropwise into the solution. After 5 min, triethylamine (2.25 g, 22.2 mmol) was added to it. The reaction mixture was stirred for 12 h. The solvent was evaporated, and 10 % HCl solution was added to the residue. The aqueous solution was extracted with DCM, the organic layer was collected and dried over Na_2SO_4 . The product was purified with column chromatography using hexane: ethyl acetate (10:4) to yield a yellowish solid. % yield = 72% (2.1 g, 5.3 mmol). ^1H NMR (CDCl_3 , 500MHz): δ 0.98 (t, 6H, CH_3), 2.3 (q, 4H, CH_2), 2.67 (s, 6H, COCH_3), 7.13 (t, 2H, ArH), 7.56 (t, 2H, ArH), 7.9 (d, 2H, ArH), 8.84 (d, 2H, ArH), 12.18 (s, 2H, NH). ^{13}C NMR (CDCl_3 , 100 MHz): δ 8.82, 25.25, 28.48, 62.18, 121.25, 122.41, 122.55, 131.51, 135.03, 140.75, 171.67, 202.55. ESI-MS [$\text{C}_{23}\text{H}_{26}\text{N}_2\text{O}_4 + \text{Na}^+$]: 417.1785 (calculated), 417.1776 (observed).

2,2-diethyl- N^1 , N^3 -bis(2-((E)-1-(hydroxyimino)ethyl)phenyl)malonamide (H_4L_2): Precursor P5 (200mg, 0.507mmole), hydroxylammonium chloride (70.46mg, 1.014mmole) and pyridine (79.1 mg, 1.014mmole) were dissolved in EtOH and the mixture was refluxed at 80 °C for 12 hrs. Then the solvent was evaporated, and water was added to the residue. The aqueous solution was extracted with DCM, the organic layer was collected and dried over Na_2SO_4 . The product was purified with the column chromatography using hexane: ethyl acetate (10:3) to yield a brownish solid. % yield = 88% (189 mg, 0.445 mmol). ^1H NMR (CDCl_3 , 500MHz): δ 0.90 (t, 6H, CH_3), 2.1 (q, 4H, CH_2), 2.19 (s, 6H, COCH_3), 7.11 (t, 2H, ArH), 7.33 (t, 2H, ArH), 7.42 (d, 2H, ArH), 8.38 (d, 2H, ArH), 8.53 (s, 2H, OH), 12.55 (s, 2H, NH). ^{13}C NMR (CDCl_3 , 100MHz): δ 8.07, 12.54, 24.22, 61.51, 121.52, 123.52, 123.83, 128.30, 129.48, 136.66, 156.85, 171.67. ESI-MS [$\text{C}_{23}\text{H}_{28}\text{N}_4\text{O}_4 + \text{Na}^+$]: 447.2003 (calculated), 447.2000 (observed).

[Cu^{II}(HL₁)(ClO₄)]•CH₃CN (1). A methanolic solution of (3 mL) of Cu (ClO₄)₂•6H₂O (0.185 g, 0.5 mmol) was slowly added to a stirring solution of H₂L₁ (0.183 g, 0.5 mmol) in 3 mL of methanol. The reaction mixture was allowed to stir at room temperature for ~1 h. The resulting reaction solvent was evaporated to dryness. The complex was purified by crystallization by diffusing diethyl ether into an acetonitrile solution of the complex at room temperature. Yield: 47 % (0.123 g). Anal. Calcd for C₂₀H₁₈CuN₅O₂ClO₄•CH₃CN, (564.44 g/mol): C, 46.81; H,

3.75; N, 14.89, Found: C, 46.83; H, 3.64; N, 15.97. IR (KBr, cm^{-1}): 3437 (br), 1591(m), 1440 (s), 1369 (s), 1274(s), 1112 (s), 1092 (s), 796 (m), 709 (m), 626 (s). ESI-MS (positive ion mode, MeOH): $m/z = 423.0739$ (LCu + H^+). UV-Vis (in MeCN): λ , nm (ϵ , $\text{M}^{-1} \text{cm}^{-1}$): 312 (4989), 517(378), 574 (338).

Complex **1-d₅** was synthesized following the same procedure as mentioned above.



Scheme S1. Synthesis of **H₂L₁-d₅**.

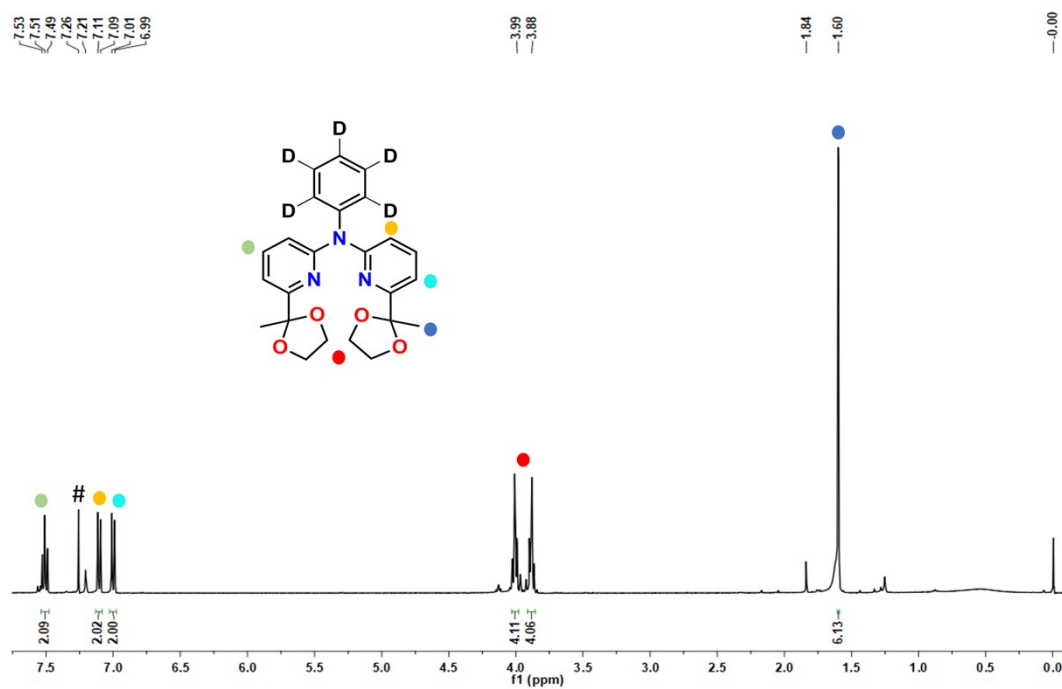


Figure S1. The $^1\text{H-NMR}$ spectrum of **P3** (400 MHz, 25 °C) in CDCl_3 .

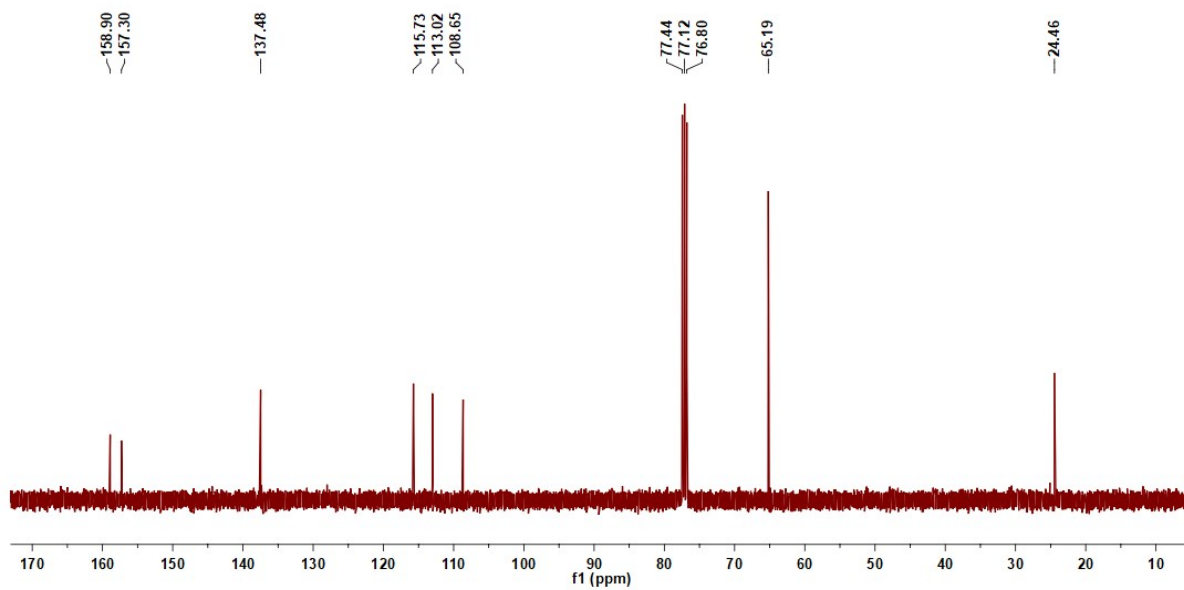


Figure S2. The $^{13}\text{C NMR}$ spectrum of **P3** (101 MHz, CDCl_3) at 25 °C.

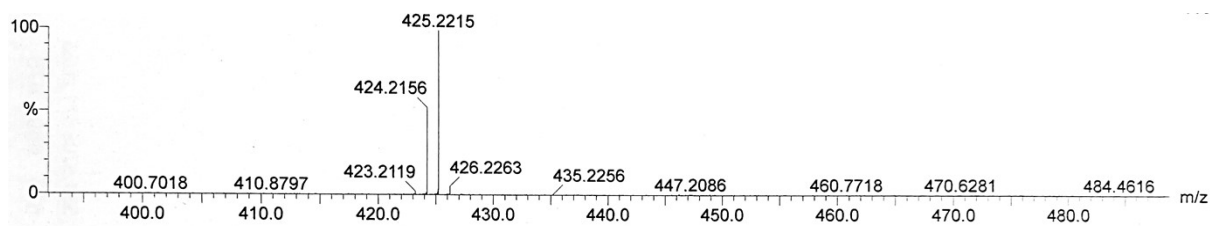


Figure S3. The ESI-mass spectrum of precursor **P3** in methanol. [$C_{24}H_{20}D_5N_3O_4 + H^+$: 425.2232 (calculated), 425.2215 (observed)]. Calculated m/z for $[P3 + H]^+$ ($C_{24}H_{20}D_5N_3O_4 + H^+$) = 425.2237; observed m/z = 425.2215.

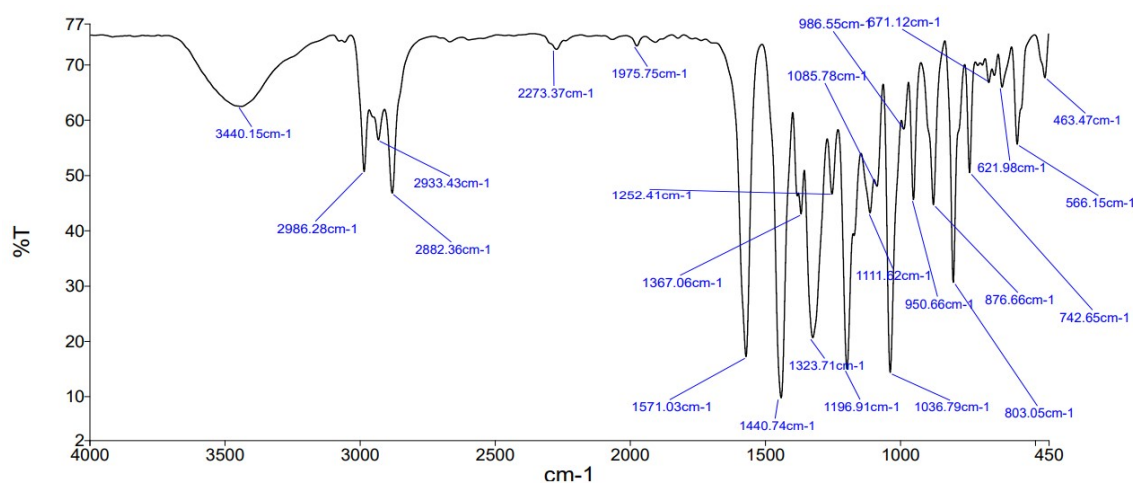


Figure S4. The FT-IR spectrum of **P3** was recorded on the KBr pellet.

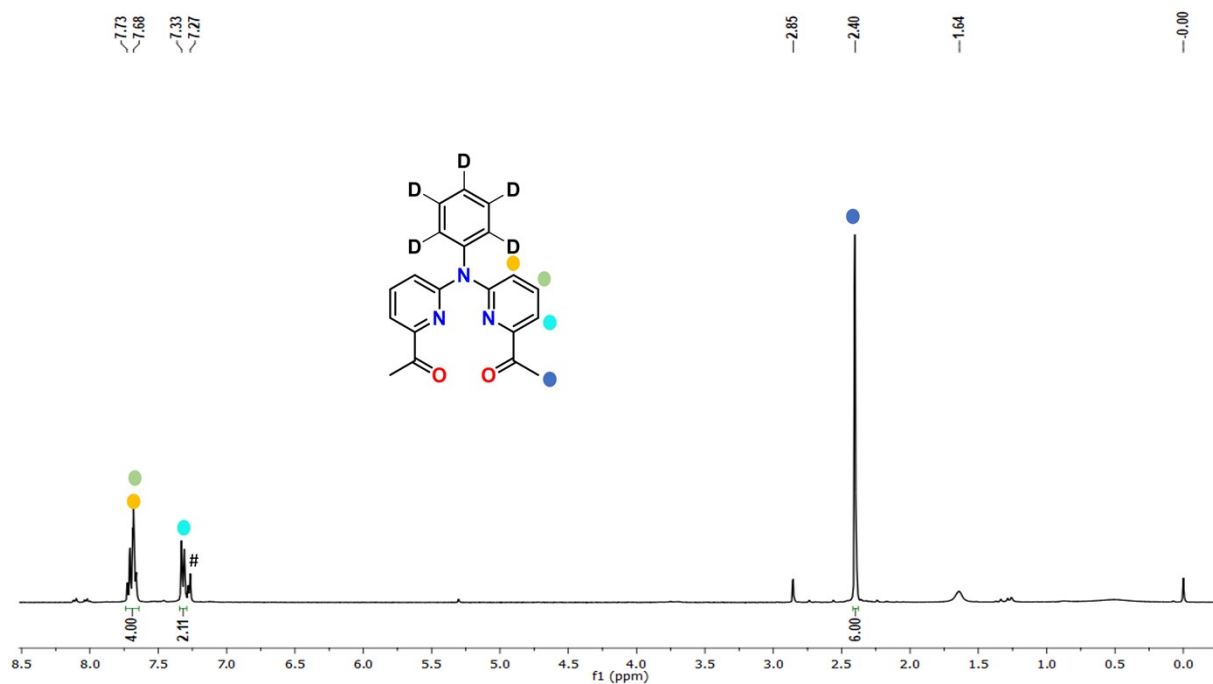


Figure S5. The 1H -NMR spectrum of **P4** in $CDCl_3$ was recorded in a 400 MHz NMR instrument at 25 °C.

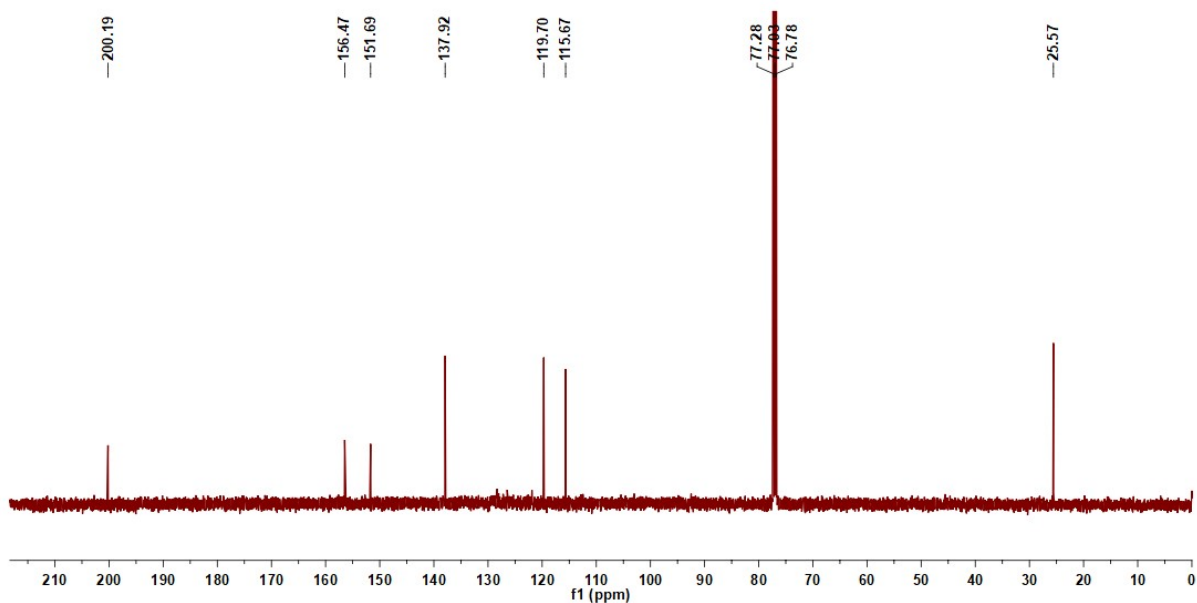


Figure S6. The ^{13}C NMR spectrum of **P4** (101 MHz, CDCl_3) at 25 °C.

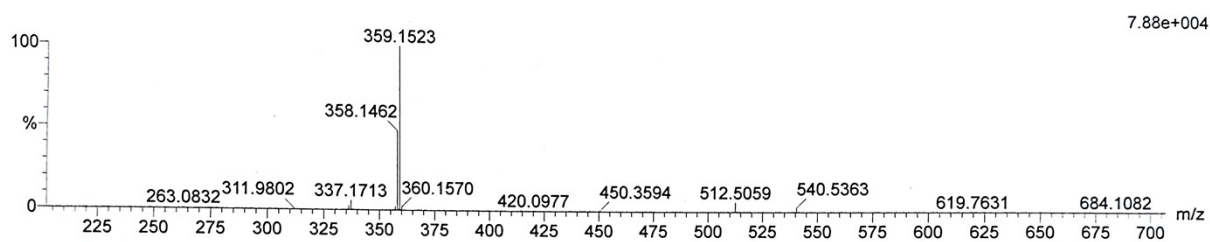


Figure S7. The ESI-mass spectrum of **P4** in methanol. Calculated m/z for $[\text{P4} + \text{Na}]^+$ ($\text{C}_{20}\text{H}_{12}\text{D}_5\text{N}_3\text{O}_2 + \text{Na}^+$) = 359.1532; observed m/z = 359.1523.

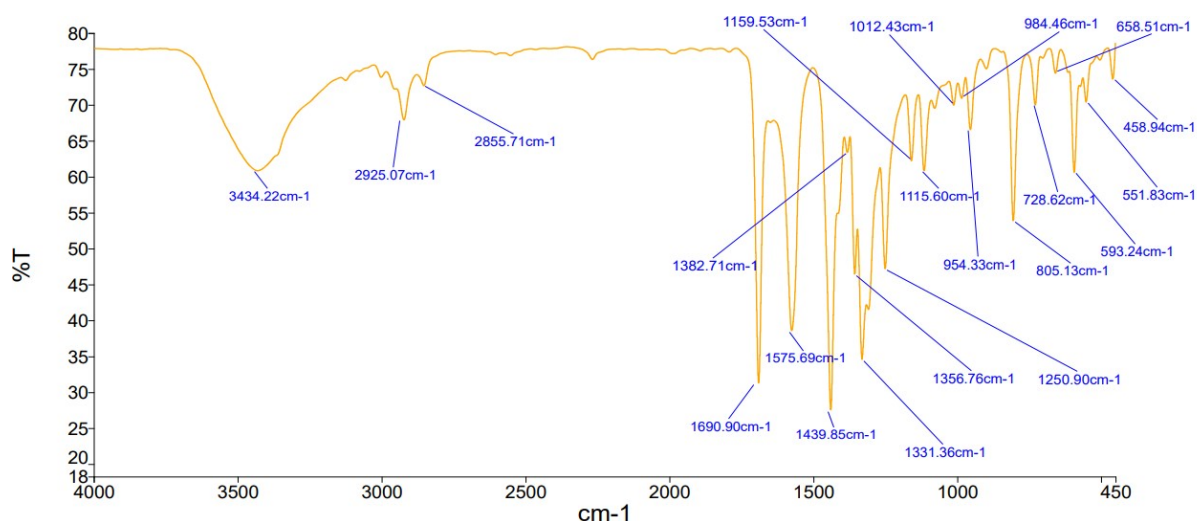


Figure S8. The FT-IR spectrum of **P4** was recorded on KBr pellet.

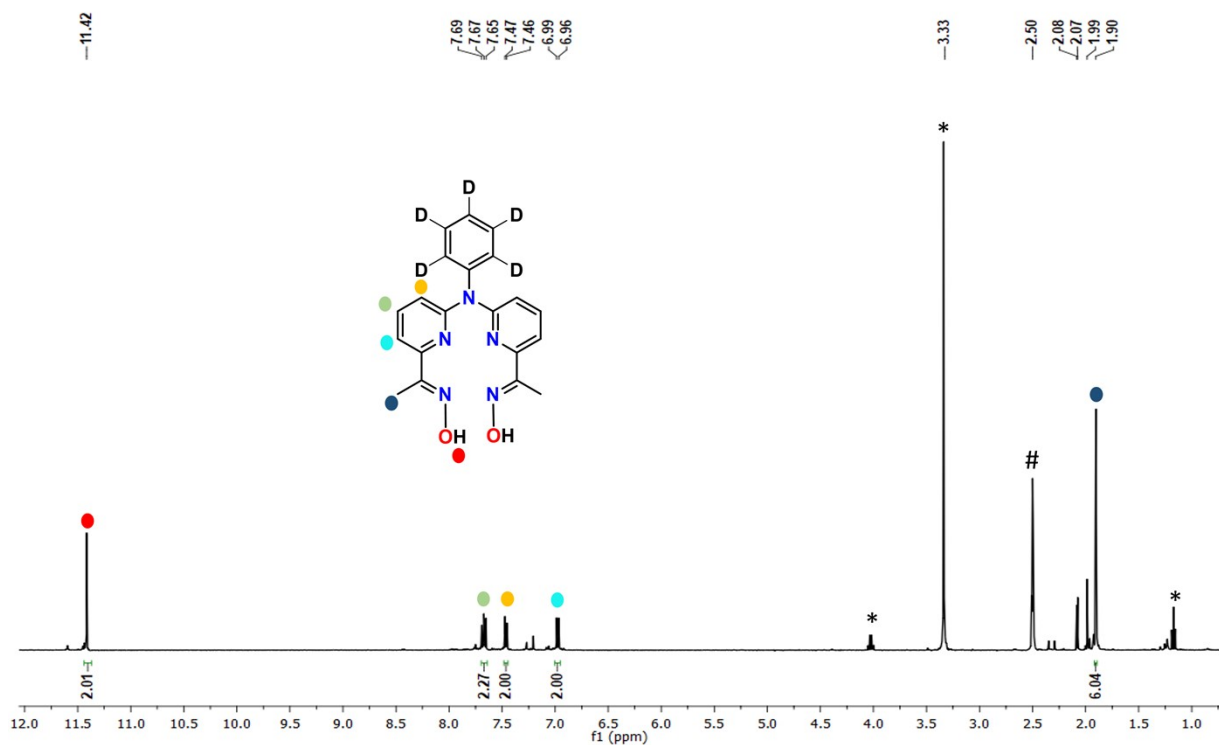


Figure S9. The 1H -NMR of $H_2L_1-d_5$ recorded in $DMSO-d_6$ in a 400 MHz NMR instrument at 25 °C. [* indicates solvent molecules]

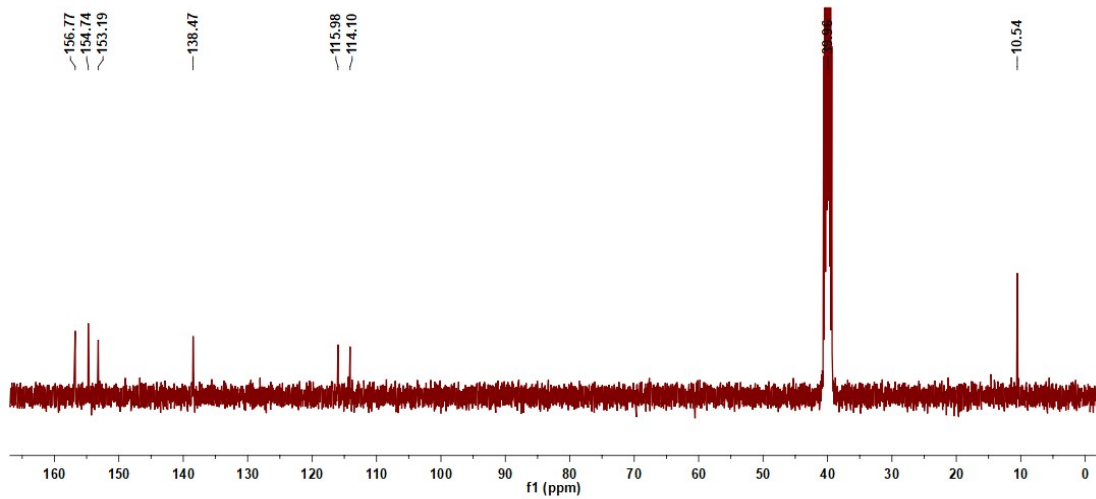


Figure S10. The ^{13}C NMR spectrum (101 MHz, in $DMSO-d_6$) of $H_2L_1-d_5$ at 25 °C.

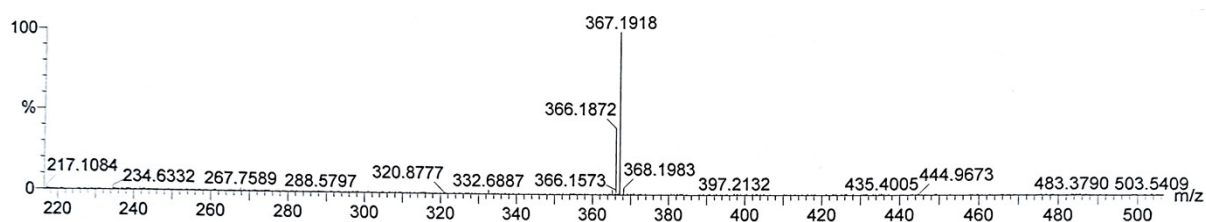


Figure S11. The ESI-mass spectrum of $H_2L_1-d_5$ in methanol. Calculated m/z for $[HL_1-d_5 + H]^+$ ($C_{20}H_{18}D_5N_5O_2 + H^+$) = 367.1931; observed m/z = 367.1918.

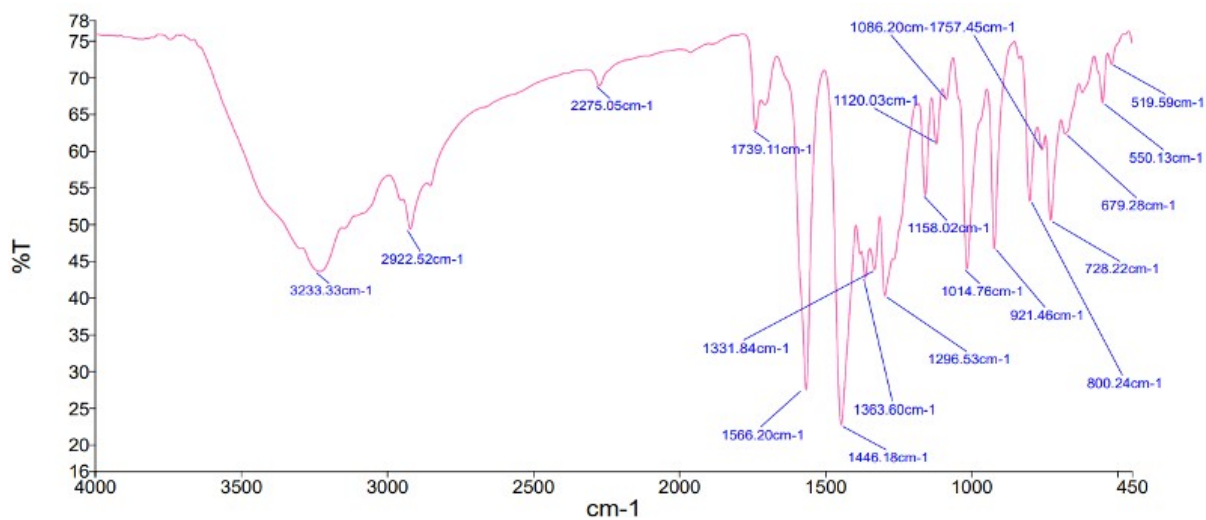


Figure S12. The FT-IR spectrum of $H_2L_1-d_5$ was recorded on a KBr pellet.

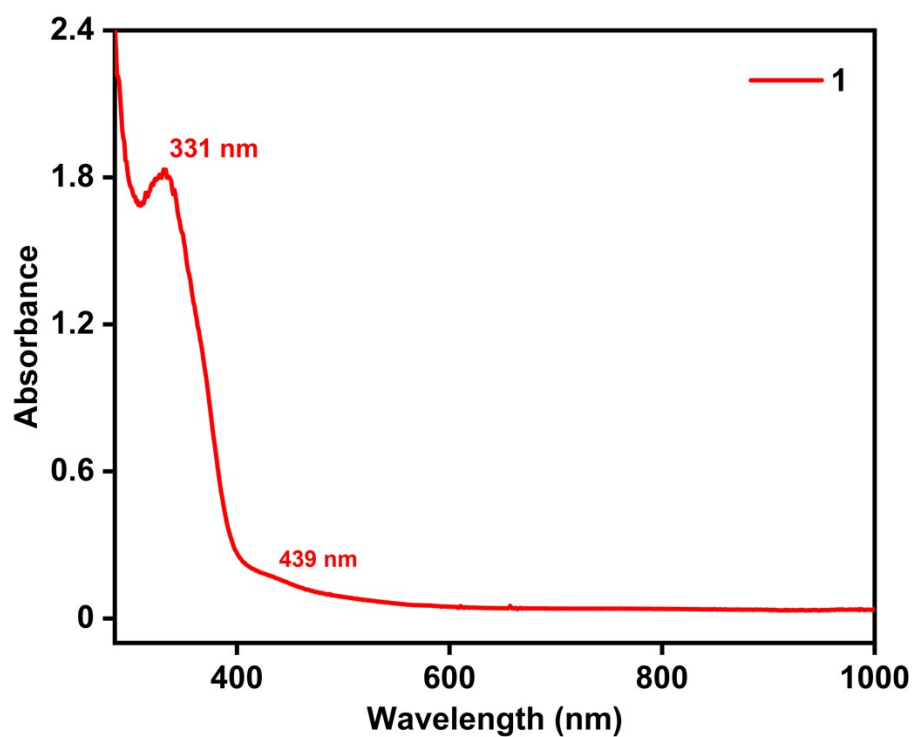


Figure S13. UV-vis spectrum of **1** (0.15 mM) in methanol at 25 °C.

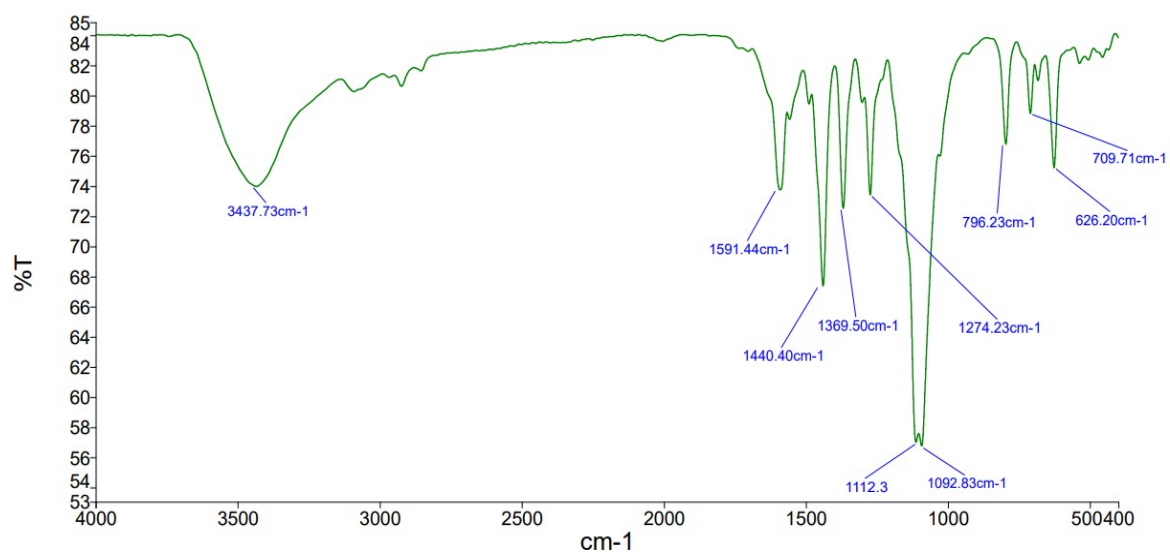


Figure S14. The FT-IR spectrum of **1** was recorded on the KBr pellet.

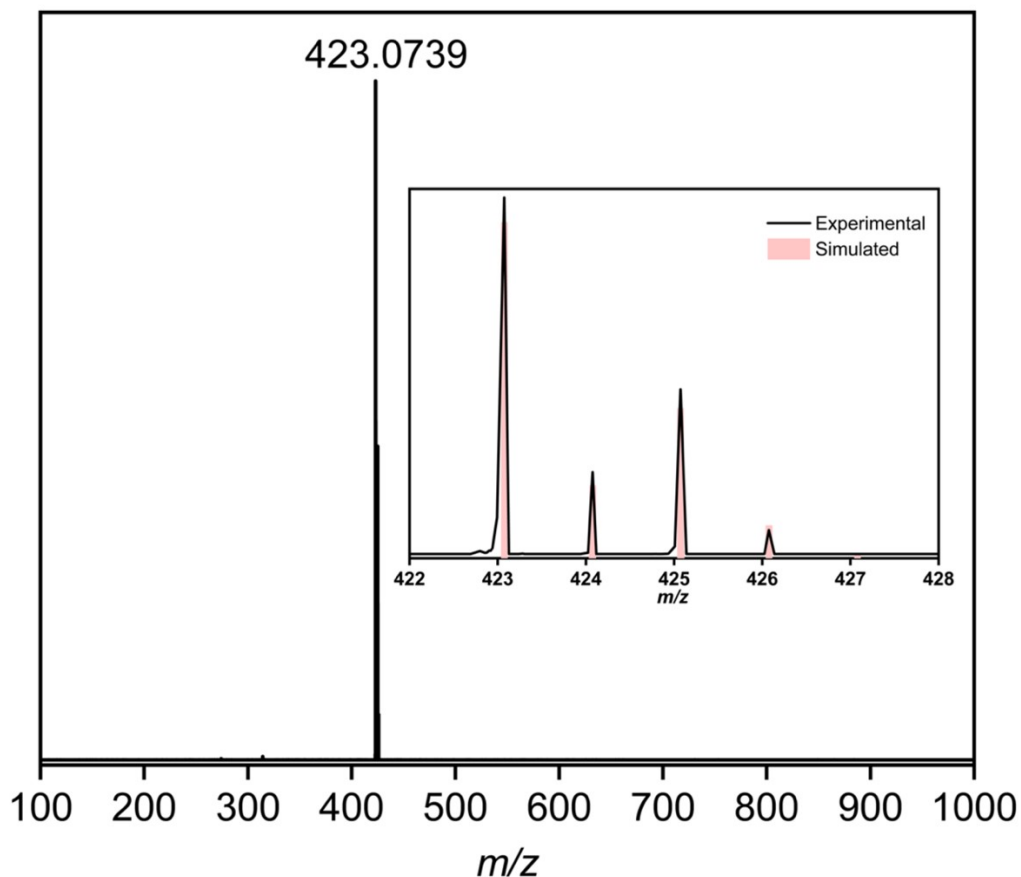


Figure S15. The ESI-mass spectrum of **1** was recorded in methanol. The inset Figure shows the experimentally obtained and theoretical isotope distribution pattern of the complex. Calculated m/z for $(HL_1)Cu]^+$ ($C_{20}H_{18}CuN_5O_2$) = 423.0756; observed m/z = 423.0739.

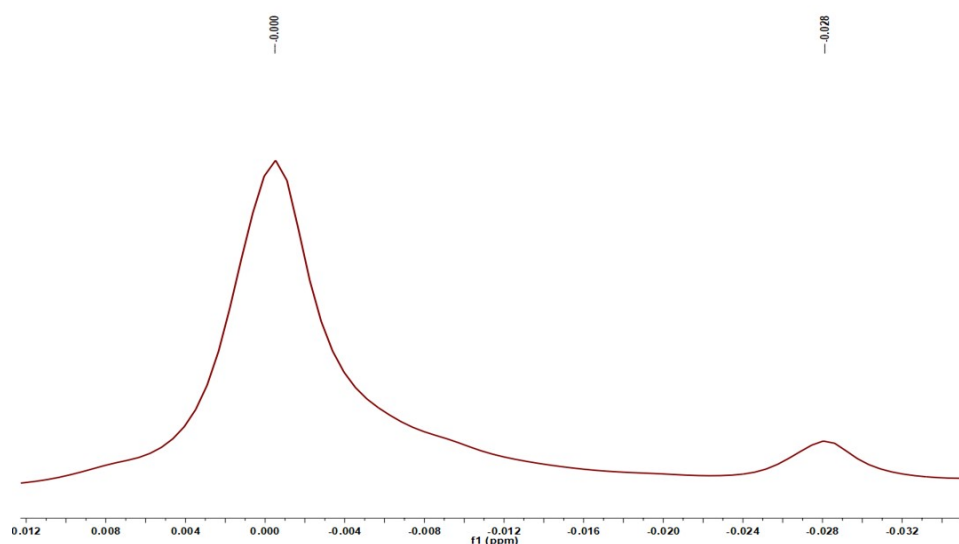


Figure S16. Measurement of the effective magnetic moment (μ_{eff}) of **1** (7.26 mM) in methanol- d_4 by Evans' method. ^1H -NMR was recorded in a 400 MHz instrument at 25 °C using hexamethyldisiloxane as an internal standard. μ_{eff} value was calculated using the difference of chemical shift of the internal standard.

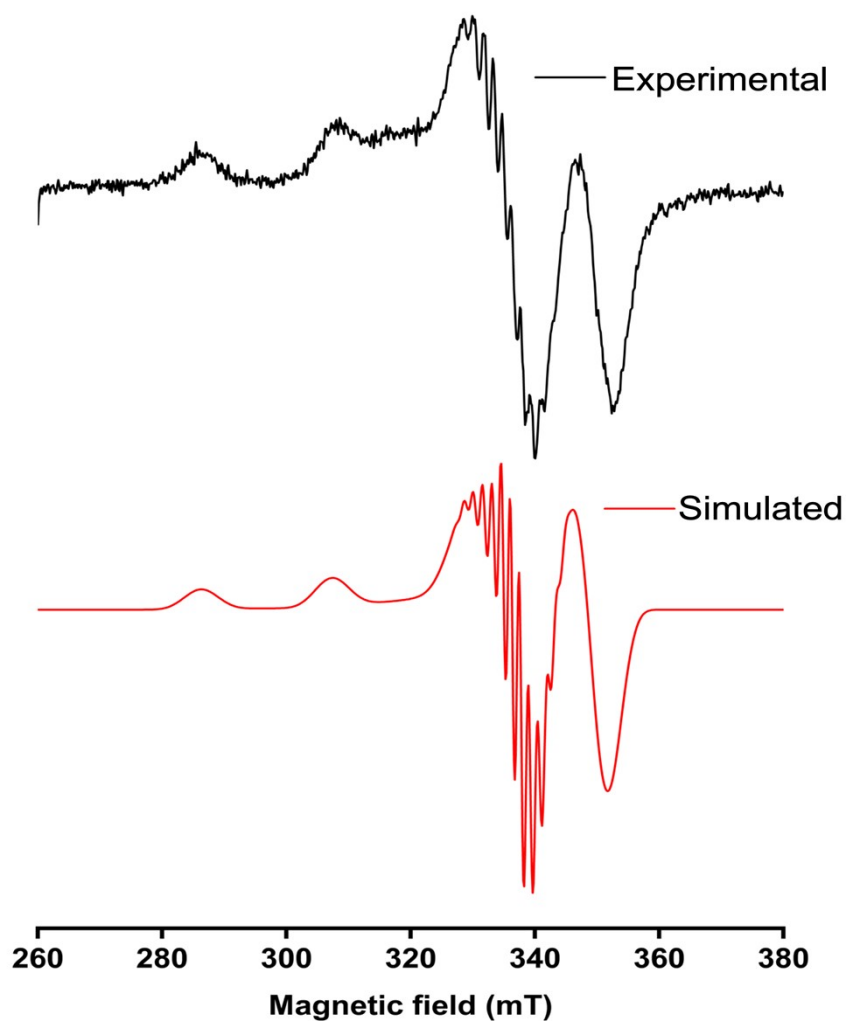


Figure S17. X-band EPR spectrum of **1** (2 mM) at 77 K (methanol) and its computer-simulated spectrum. EPR measurement experimental conditions: Frequency = 9.628961 GHz, Power = 2.01 mW, Modulation frequency = 100 kHz, Modulation amplitude = 4.91 G.

Simulated parameters: 2.045 (g_x), 2.09 (g_y), and 2.165 (g_z); 20 G (A^{Cu_x}), 30 G (A^{Cu_y}), 210 G (A^{Cu_z}), 14 G (A^{N_x}), 15.3 G (A^{N_y}), 13 G (A^{N_z})

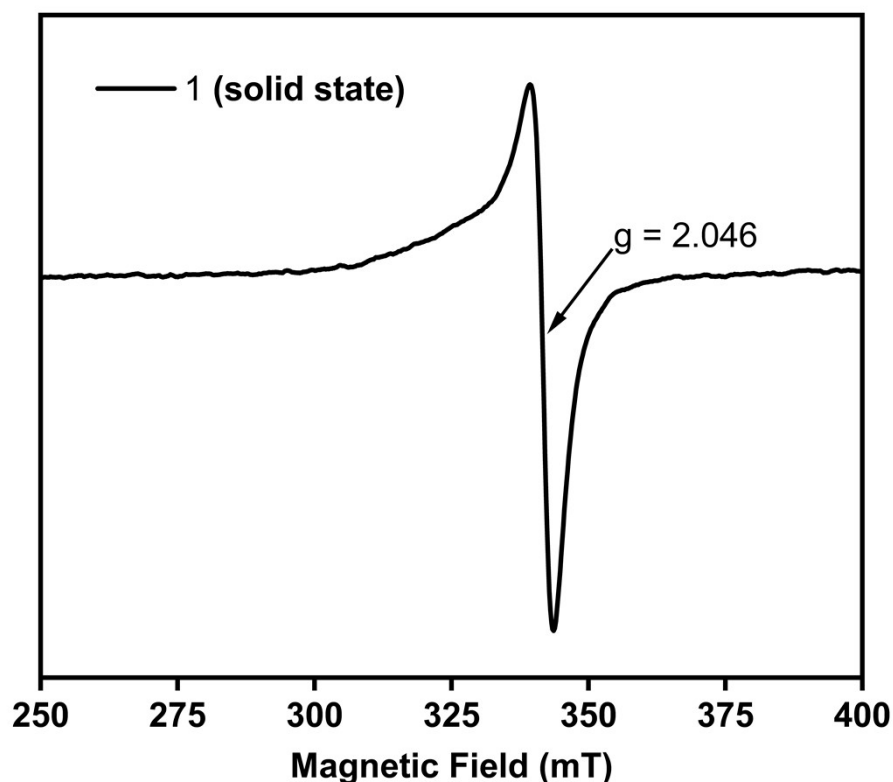


Figure S18. X-band EPR spectrum of **1** at room temperature. EPR measurement experimental conditions: Frequency = 9.783718 GHz, Power = 3.88 mW, Modulation frequency = 100 kHz, Modulation amplitude = 0.5 G.

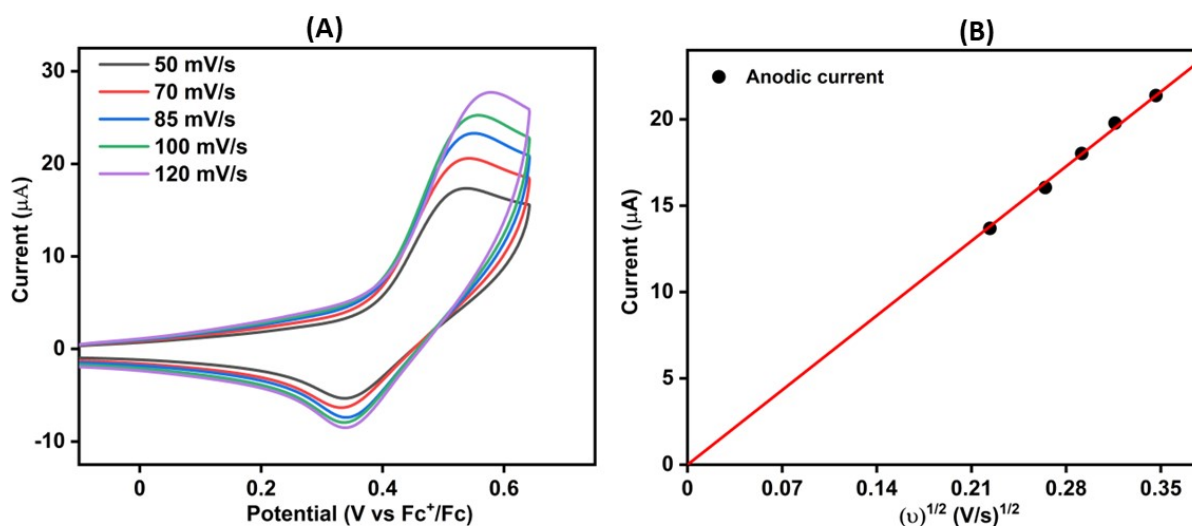


Figure S19. CV of **1** (0.5 mM) at different scan rates in methanol. The data was recorded using a glassy carbon working electrode, Pt wire counter electrode, and Ag/AgCl in saturated KCl as the reference electrode. Potential values were converted to Fc^+/Fc couple. (B). A plot of anodic/cathodic current vs. $v^{1/2}$.

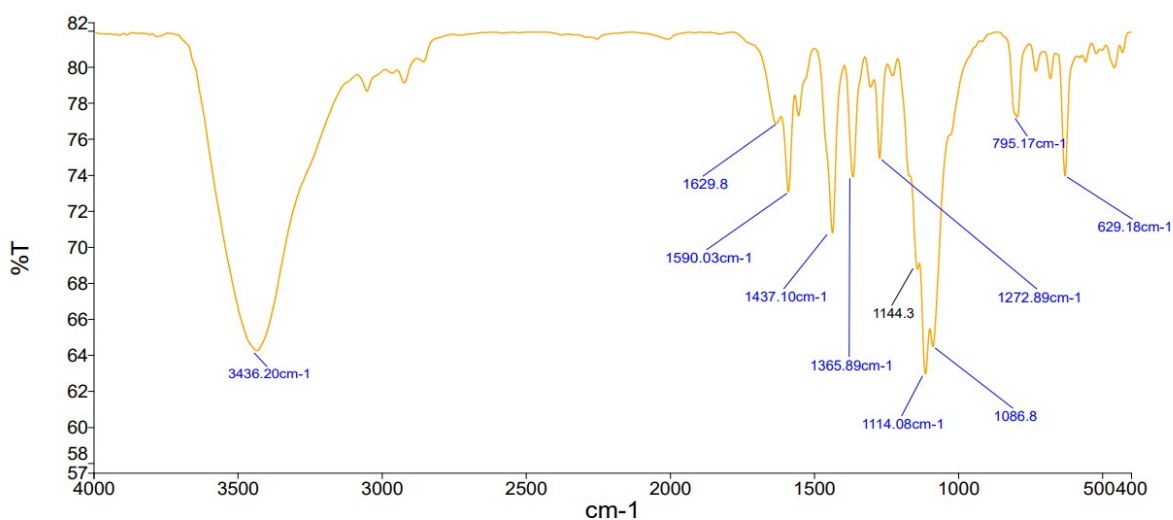


Figure S20. The FT-IR spectrum of 1-d₅ was recorded on the KBr pellet.

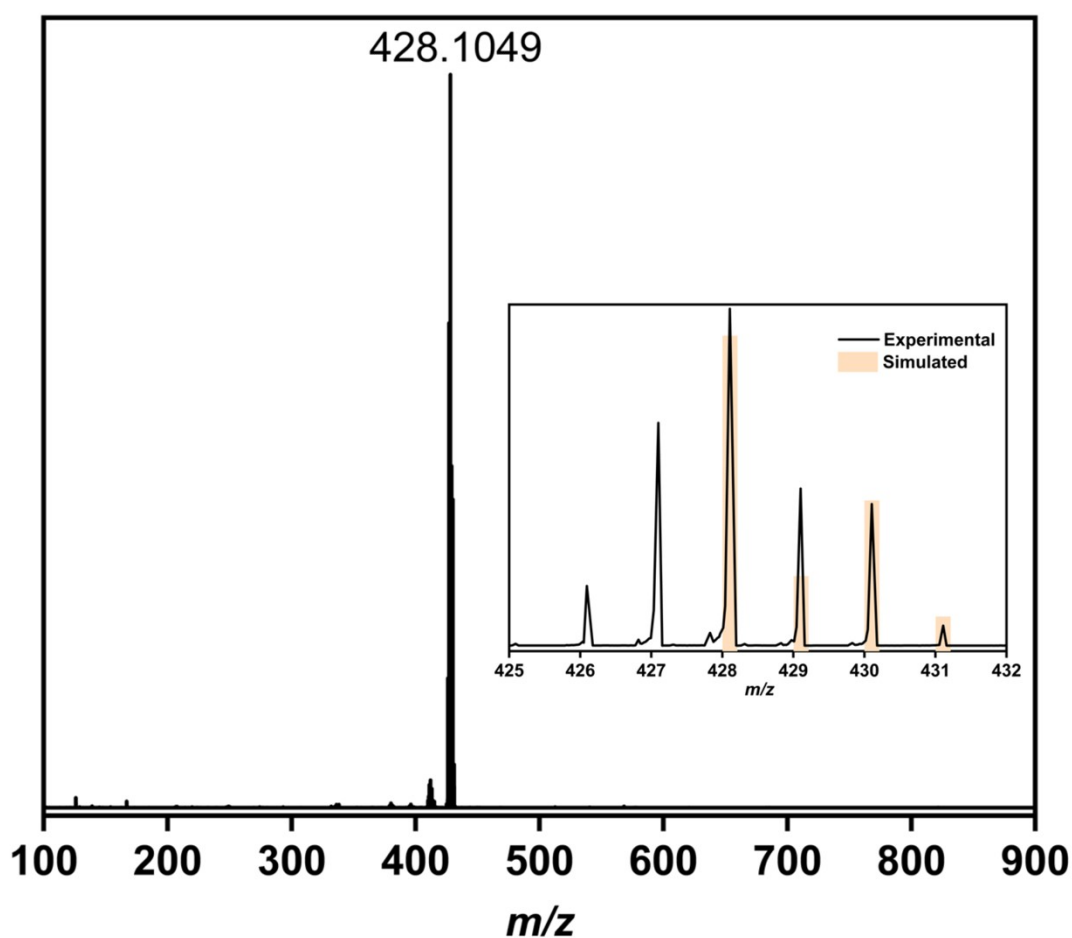


Figure S21. The ESI-mass spectrum of 1-d₅ was recorded in methanol. The inset Figure shows the experimentally obtained and theoretical isotope distribution pattern of the complex. Calculated m/z for $(HL_1-d_5)Cu]^+$ ($C_{20}H_{13}D_5CuN_5O_2$) = 428.1070; observed m/z = 428.1049. The peaks observed at 427.0996 and 426.0937 likely correspond to the fragmentation of the parent peak.

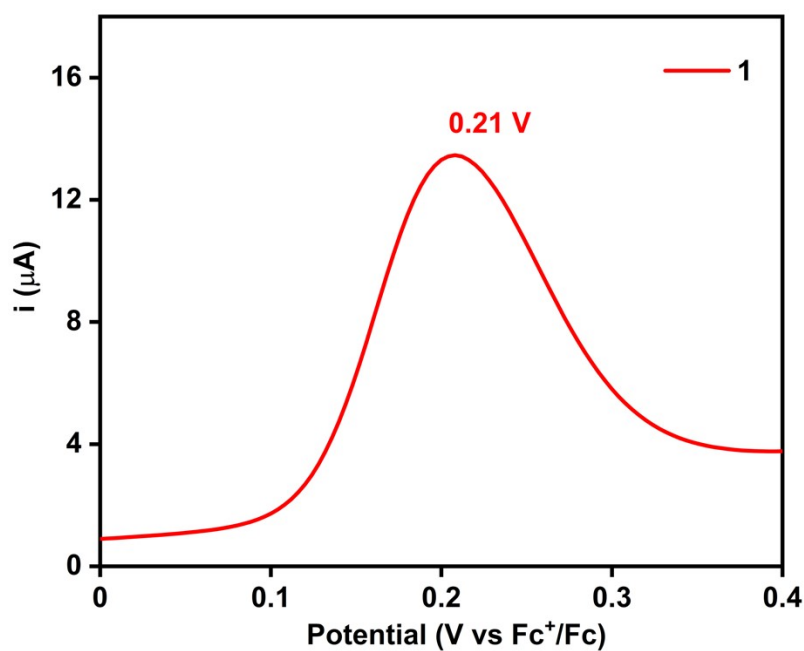


Figure S22. DPV of **1** in acetonitrile at 25 °C. A glassy carbon working electrode and Pt wire counter electrode were used during the measurements. An excess of $n\text{Bu}_4\text{NClO}_4$ was used as the supporting electrolyte.

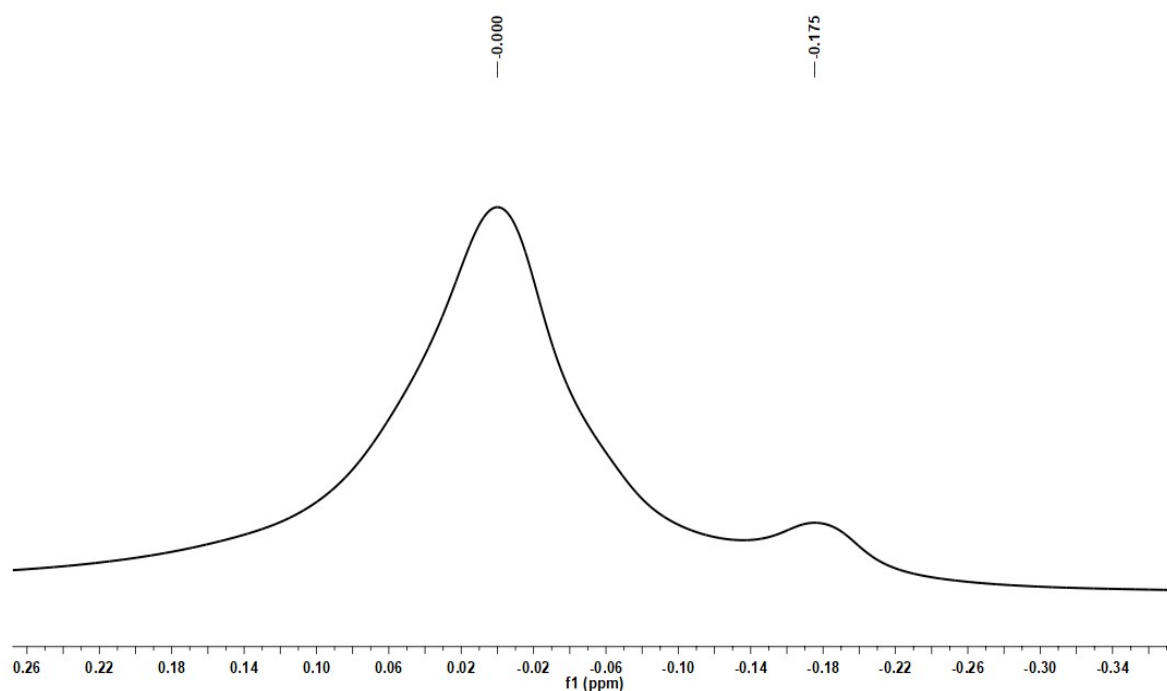


Figure S23. Measurement of the effective magnetic moment (μ_{eff}) of **1-ox** (10.99 mM) in methanol- d_3 by Evans' method. The ^1H -NMR spectrum was recorded in a 400 MHz instrument at -40 °C using hexamethyldisiloxane as an internal standard. μ_{eff} value was calculated using the difference of chemical shift of the internal standard.

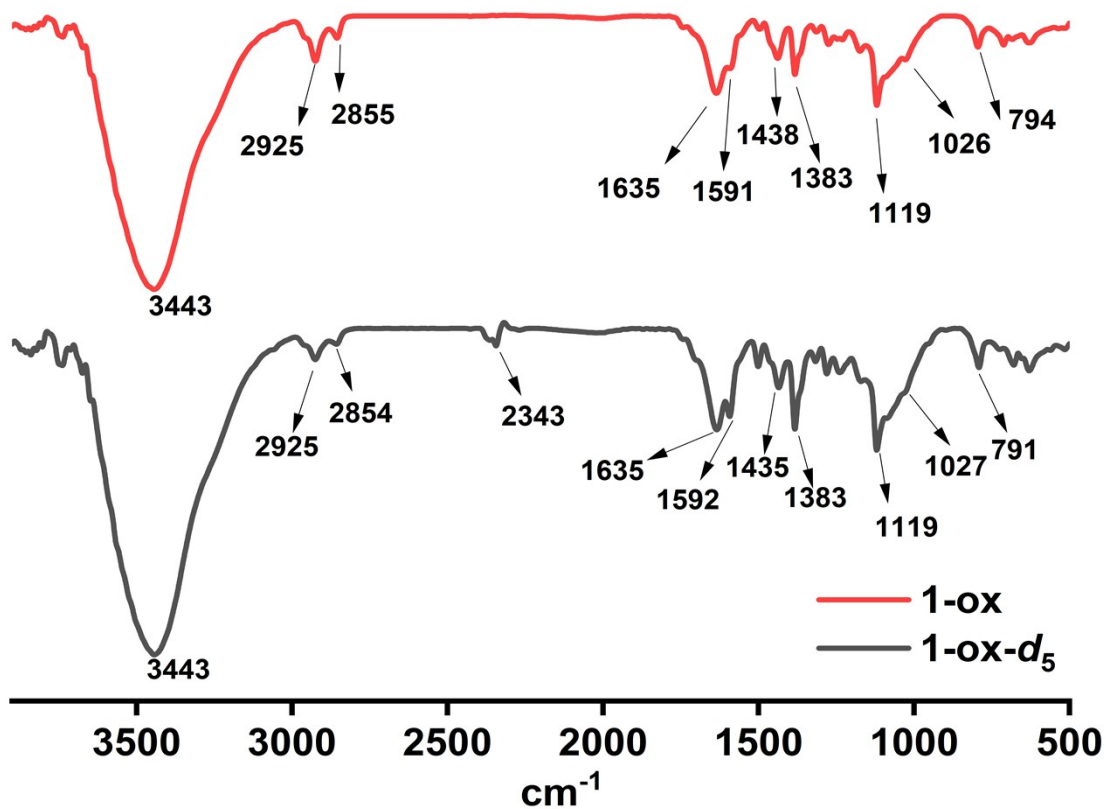


Figure S24. The FT-IR spectrum of 1-ox and 1-ox-*d*₅ was recorded on the KBr palette.

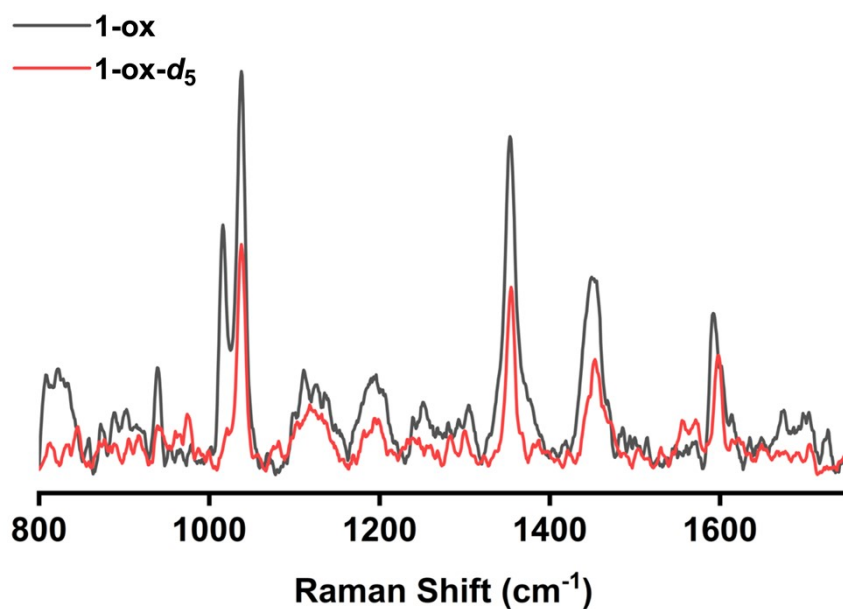


Figure S25. Raman spectrum of 1-ox and 1-ox-*d*₅ in methanol was recorded using a 785 nm laser.

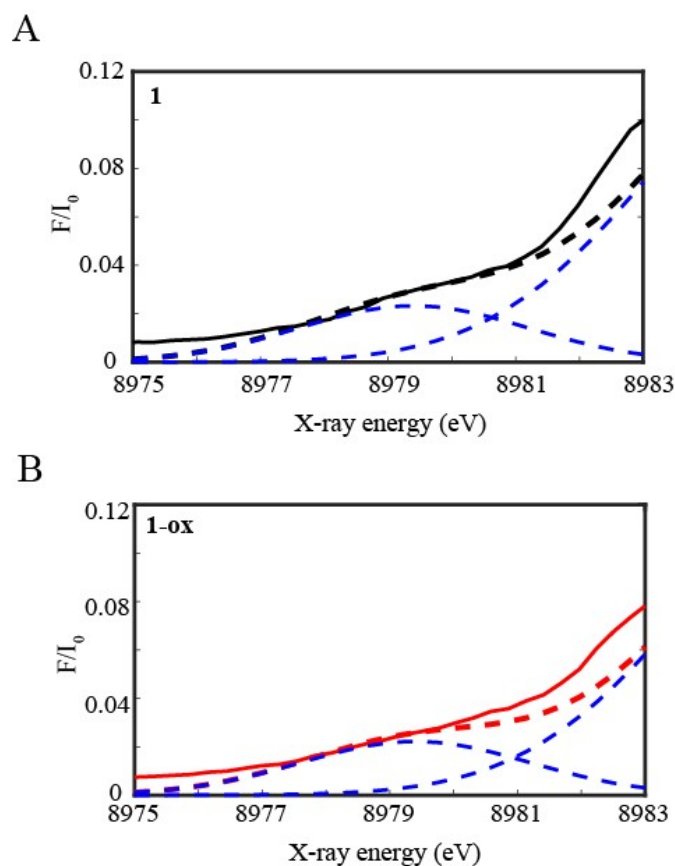


Figure S26. Zoom-in of the pre-edge regions together with the respective fits shown in dashed blue of A. **1** and B. **1-ox**. The dashed lines correspond to the step and gaussian functions used to fit the pre-edge peaks whereas the blue dashed line correspond to the summed overall fit.

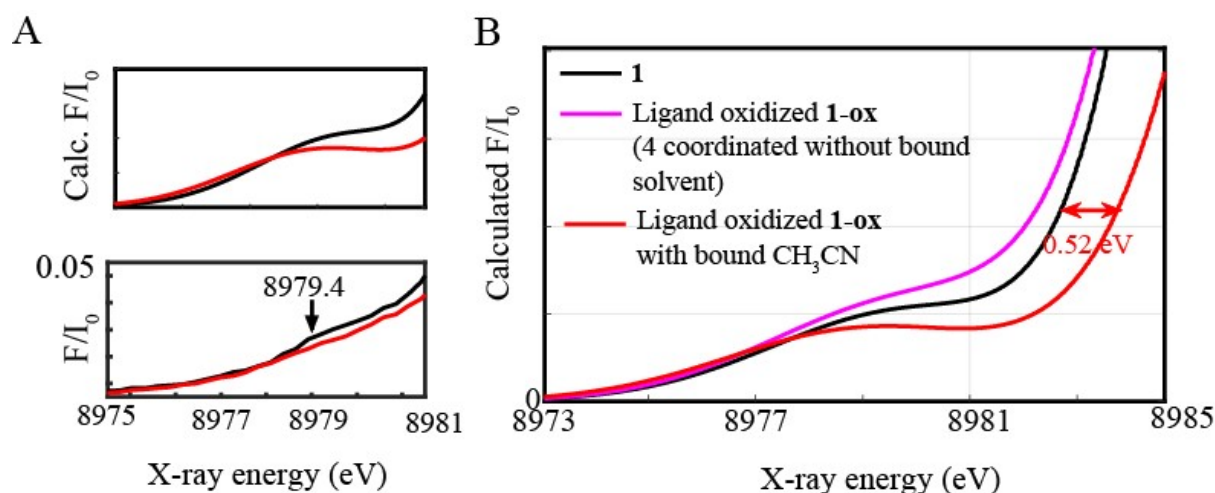


Figure S27 A. Zoom-in of the calculated (top) and experimental (bottom) pre-edge regions of **1** (black) and **1-ox** (red) B. Calculated pre-edge and rising edge XANES of calculated models of **1**, 4-coordinated ligand oxidized **1-ox** without bound solvent molecules, Five-coordinated ligand oxidized **1-ox** with a bound acetonitrile molecule.

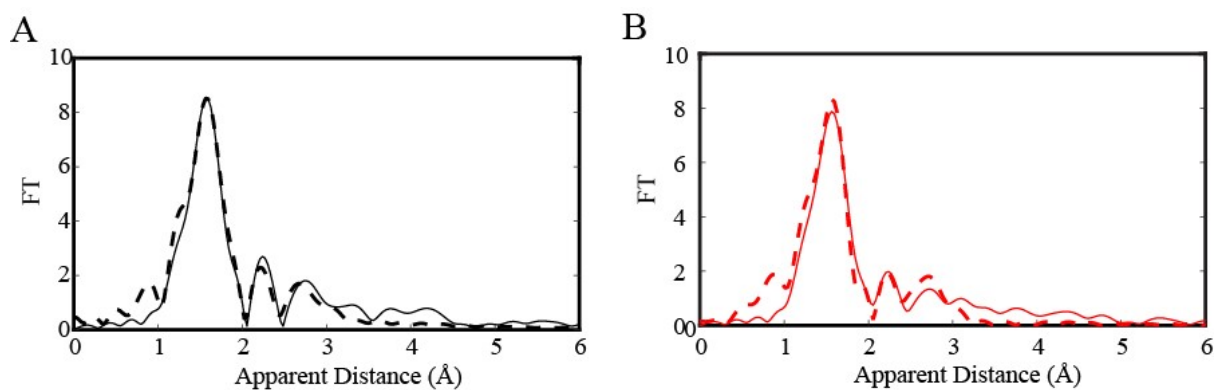


Figure S28. Fourier transforms of k^3 -weighted Cu EXAFS for **A. 1** (solid black line) and its corresponding fit (Fit 3, **Table S3**) and **B. Ligand oxidized 1-ox** (solid red line) and its corresponding fit (Fit 6, **Table S3**).

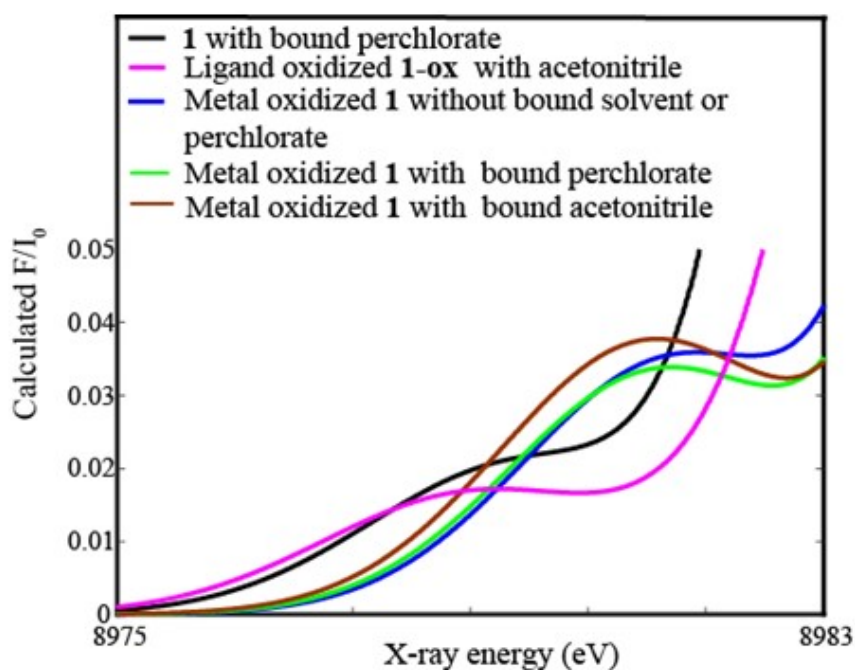
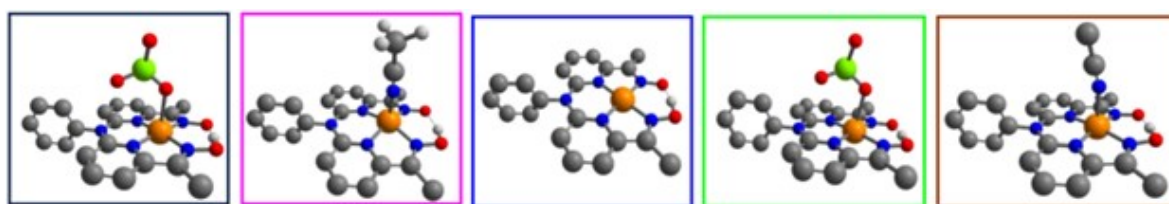


Figure S29 Top. Calculated Pre-edge models. Bottom. Calculated pre-edge for **1** (with bound perchlorate), Ligand oxidized **1-ox** (with bound acetonitrile), metal oxidized **1** without bound solvent or perchlorate, metal oxidized **1** with bound acetonitrile, and metal oxidized **1** with bound acetonitrile.

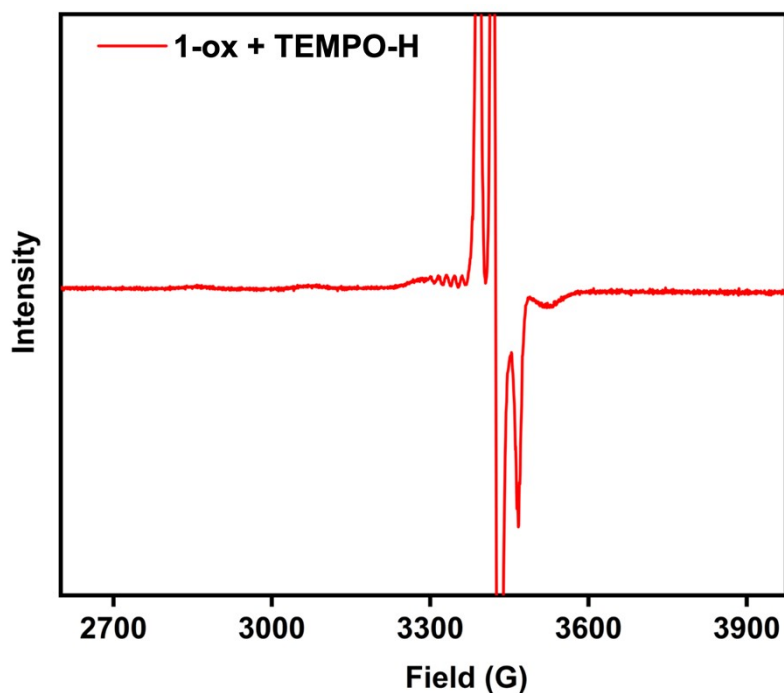


Figure S30. The X-band EPR spectrum of the reaction mixture was obtained after the addition of one equivalent TEMPOH to **1-ox** in methanol at $-40\text{ }^{\circ}\text{C}$. The EPR data was recorded at the liquid nitrogen temperature.

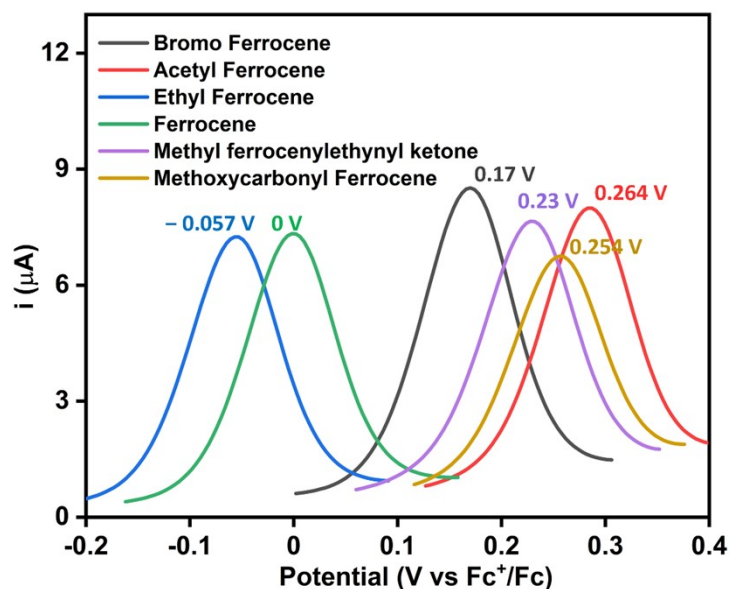
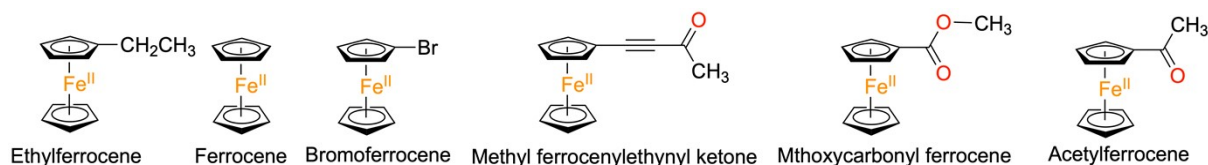


Figure S31. DPV data of different ferrocene derivatives showing one-electron oxidation potentials in methanol. The data was recorded in methanol at $25\text{ }^{\circ}\text{C}$ using a glassy carbon working electrode and Pt wire counter electrode. $n\text{Bu}_4\text{NClO}_4$ was used as the supporting electrolyte.

Table S6. ET rate constant values of **1-ox** at $-60\text{ }^{\circ}\text{C}$ in methanol. The E_{ox} values of the ferrocene derivatives were measured at $25\text{ }^{\circ}\text{C}$.

Substrate	E_{ox} (vs. Fc^+/Fc)	k_{et} ($\text{M}^{-1}\text{ s}^{-1}$)
Ethylferrocene	-0.05	2.5×10^3
Ferrocene	0	1.3×10^3
Bromoferrocene	0.17	96
Methyl ferrocenylethynyl ketone	0.23	24.3
(methoxycarbonyl) ferrocene	0.25	20.7
Acetyl ferrocene	0.28	11

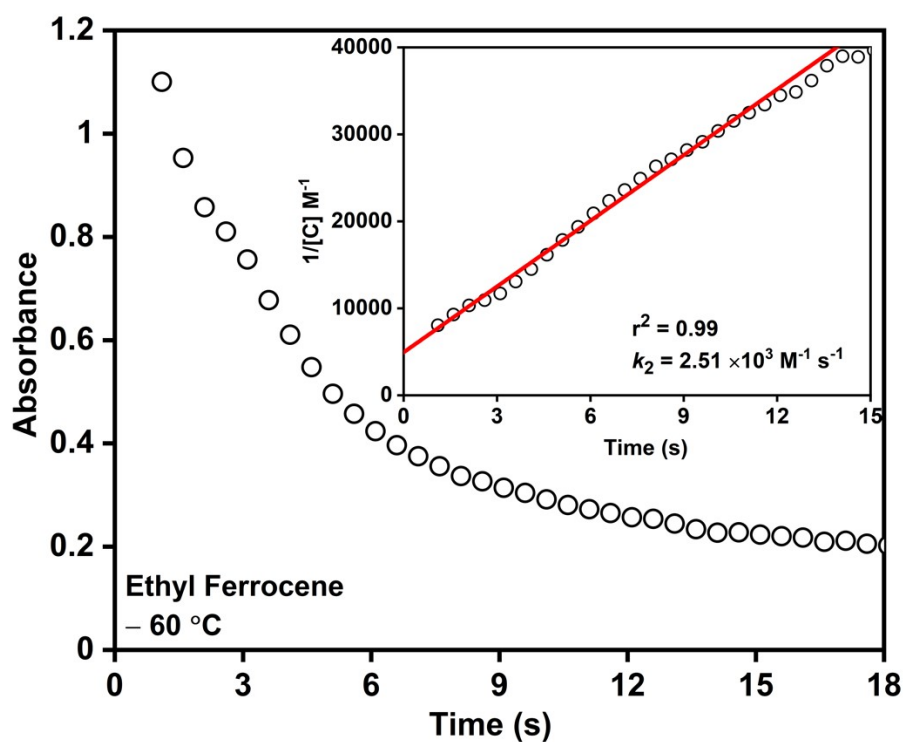


Figure S32. Time trace at 543 nm upon addition of one equivalent of ethyl ferrocene to **1-ox** at $-60\text{ }^{\circ}\text{C}$. [inset: Plot of $1/[\mathbf{1-ox}]$ vs. time for determining second order rate constant value at $-60\text{ }^{\circ}\text{C}$.]

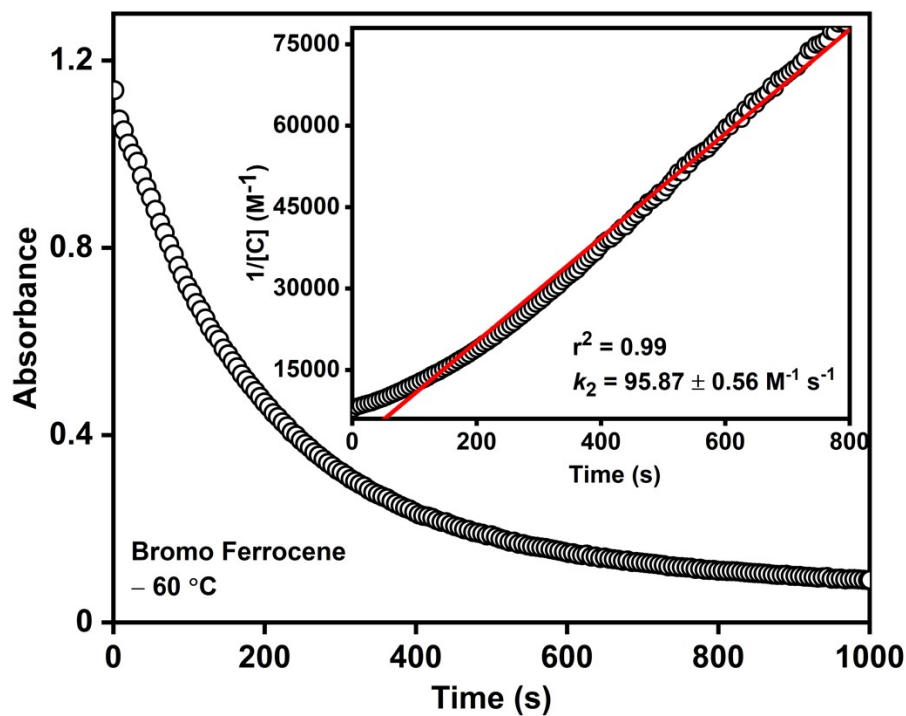


Figure S33. Time Trace at 543 nm upon addition of one equivalent of bromo ferrocene to **1-ox** at $-60\text{ }^{\circ}\text{C}$. [inset: Plot of $1/[1\text{-ox}]$ vs. time for determining second order rate constant value at $-60\text{ }^{\circ}\text{C}$.]

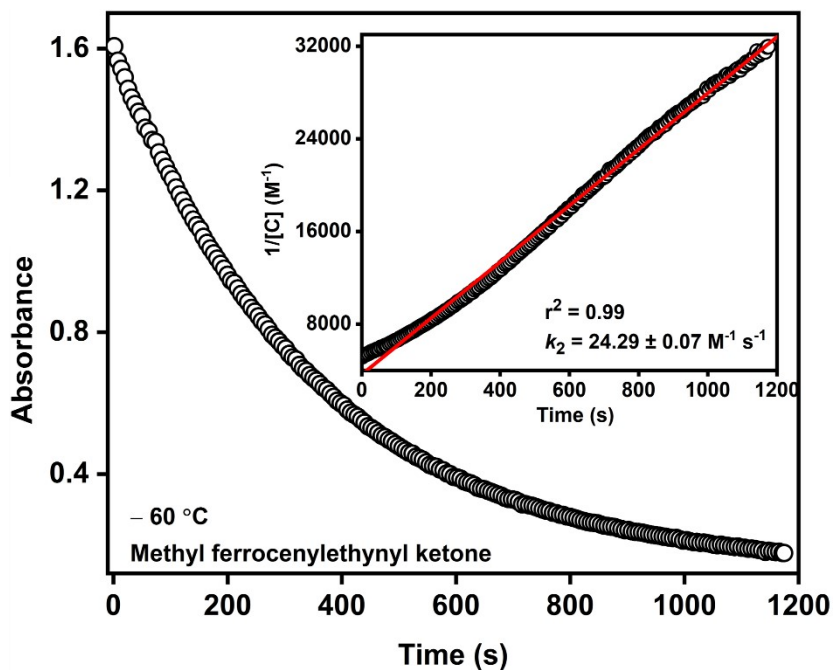


Figure S34. Time trace at 543 nm upon addition of one equivalent of methyl ferrocenylethynyl ketone to **1-ox** at $-60\text{ }^{\circ}\text{C}$. [inset: Plot of $1/[1\text{-ox}]$ vs. time for the determination of second order rate constant value at $-60\text{ }^{\circ}\text{C}$.]

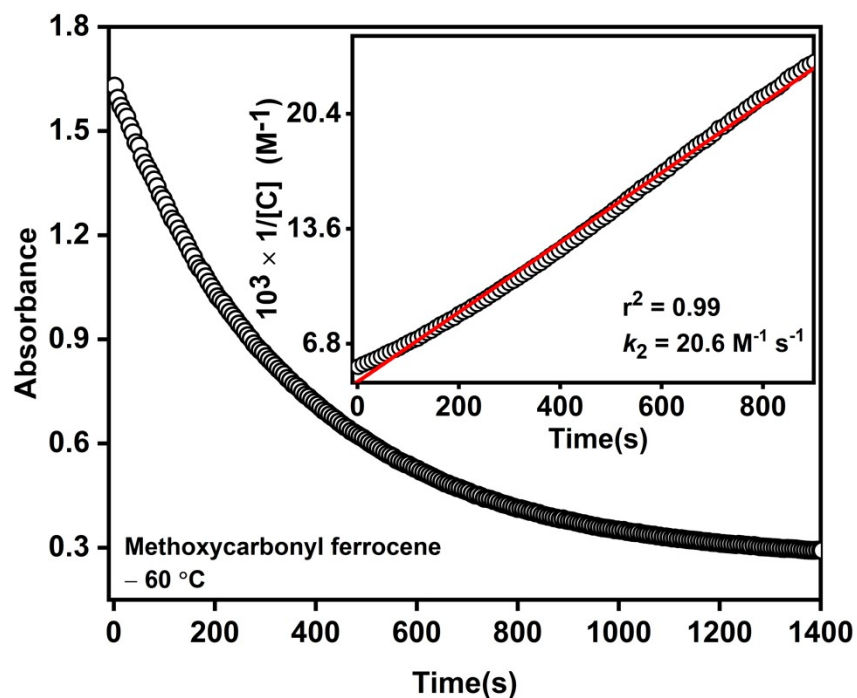


Figure S35. Time trace at 543 nm upon addition of one equivalent of (methoxycarbonyl) ferrocene to **1-ox** at $-60\text{ }^{\circ}\text{C}$. [inset: Plot of $1/[1\text{-ox}]$ vs time for determining second order rate constant value at $-60\text{ }^{\circ}\text{C}$.]

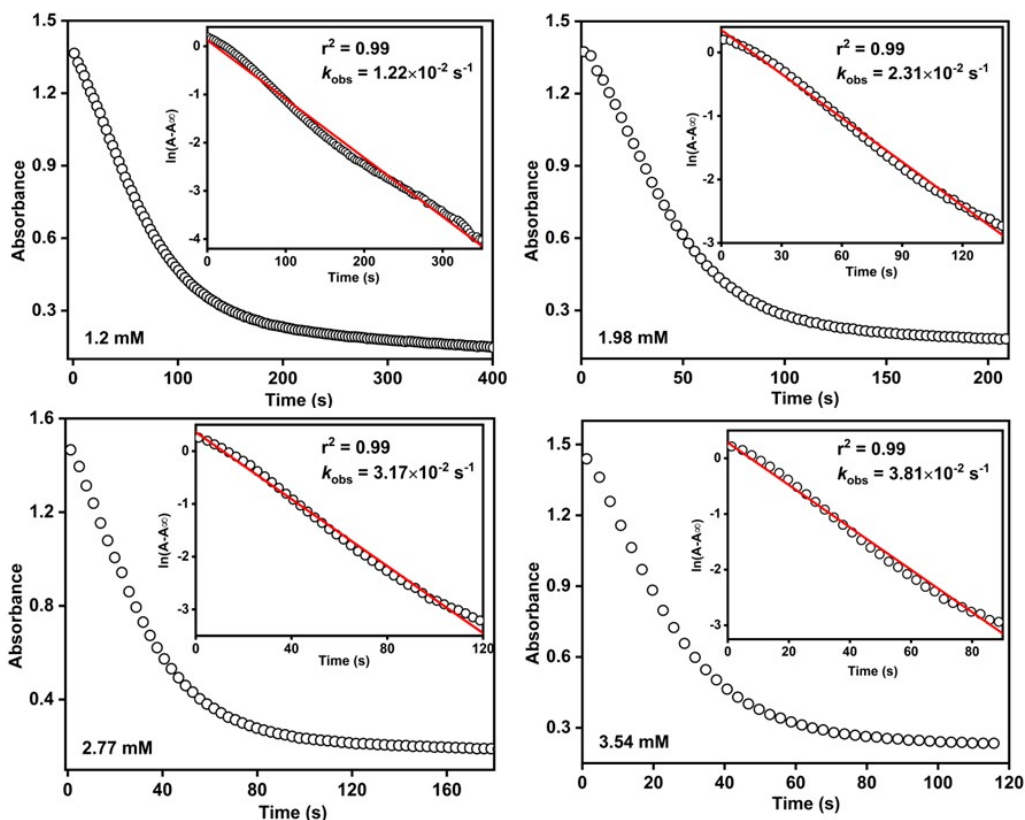


Figure S36. Time trace at 543 nm for the reaction of **1-ox** with acetyl ferrocene (1.2 mM, 1.98 mM, 2.77 mM, and 3.54 mM) at $-60\text{ }^{\circ}\text{C}$. [inset: Plot of $\ln(A-A_{\infty})$ vs. time (s) for the determination of pseudo-first-order rate constant (k_{obs}) value at $-60\text{ }^{\circ}\text{C}$.]

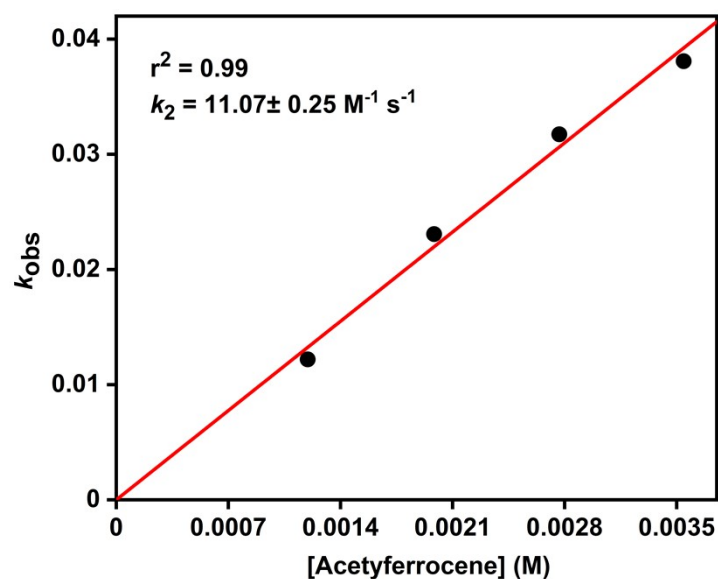


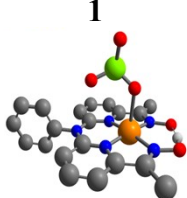
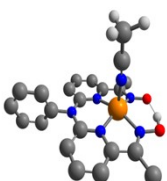
Figure S37. A plot of k_{obs} (s^{-1}) vs. [acetylferrocene] for the determination of second order rate constant (k_2) value for the reaction of **1-ox** with acetylferrocene at -60 °C.

Table S7. Summary of the bond distances of calculated Cu-based complexes. Bond distances are in Å.

Complexes	Cu-N ₁	Cu-N ₂	Cu-N ₃	Cu-N ₄	Cu-O (Perchlorate)	Cu-N (Acetonitrile)	Cu-O (Methanol)
1 with perchlorate	1.931 81	1.951 27	1.9568 6	1.9461 0	2.44430		
1 without solvent or perchlorate	1.941 36	1.951 78	1.9500 6	1.9276 0			
1 with bound acetonitrile	1.936 79	1.956 71	1.9592 4	1.9557 8		2.36773	
Ligand oxidized 1-ox without bound solvent or perchlorate	1.932 36	1.965 24	1.9650 0	1.9474 0			
Ligand oxidized 1-ox with bound perchlorate	1.941 78	1.962 10	1.9700 3	1.9554 1	2.30678		
Ligand oxidized 1-ox with	1.968 55	1.972 09	1.9887 1	1.9803 5		2.06838	

bound acetonitrile							
Metal oxidized 1 without bound perchlorate or solvent	1.885 22	1.923 54	1.9170 7	1.8975 3			
Metal oxidized 1 with perchlorate	1.887 52	1.923 94	1.9204 9	1.8988 1	2.39244		
Metal oxidized 1 with acetonitrile	1.895 22	1.922 17	1.9236 4	1.9037 0		2.28676	

Table S8. Electronic energies and LUMO-HOMO gaps energies at 298.15 K of **1** and **1-ox**

Complex	Electronic energy (Eh) kcal/mol	LUMO - HOMO gap (eV)
1 	- 3275.5632916 22529	3.4690164028
1-ox 	- 2647.1320064 82481	1.557455926

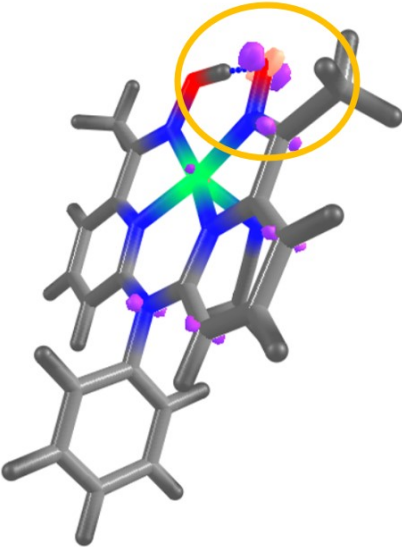
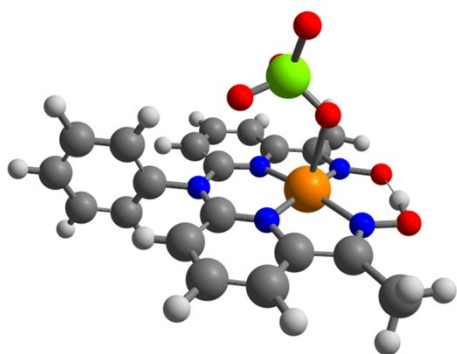
<p>Electron density differences between 1 and 1-ox showing most of the spin density distributions to be around the iminoxyl radical.</p>	
<p>ΔE (kcal/mol) between 1-ox and 1</p>	<p>628.43128</p>

Table S9. Electronic energies of the starting Cu^{II} doublet, Cu^{II} radical triplet species, and Cu^{III} singlet species.

	Electronic energy (Eh)
Cu ^{II} starting doublet species (1)	-2971.25780
Cu ^{II} radical triplet species	-2971.03479
Cu ^{III} singlet	-2971.06202
	ΔE (kcal/mol)
Triplet-doublet	0.22301
Singlet-doublet	0.19578

The following Tables present the DFT optimized coordinates that were obtained using the BP-86¹⁴ functional, the CPCM model, and the atom-pairwise Grimme dispersion correction with the Becke-Johnson damping scheme (D3BJ)^{16, 23}.

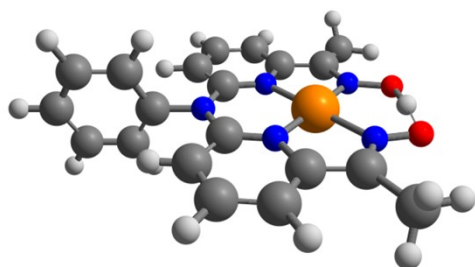
Table S10. 1 with perchlorate



29	5.578649000	9.066882000	4.317758000
8	8.054630000	10.558265000	4.698605000
8	7.431166000	8.900713000	6.501450000
7	2.773109000	8.459755000	2.817299000
1	7.873571000	9.867446000	5.507669000
7	4.746448000	9.811060000	2.723718000
7	4.058067000	7.967906000	4.778157000
7	6.280393000	8.480908000	6.041608000
7	6.963572000	10.392491000	3.925276000
6	3.572356000	9.434669000	2.199358000
6	5.510768000	7.618265000	6.666221000
6	4.270630000	7.297523000	5.952577000
6	1.584420000	8.078062000	2.073334000
6	2.977425000	7.750678000	4.016104000
6	1.678506000	7.056191000	1.128494000
1	2.636683000	6.560694000	0.969526000
6	5.528060000	10.766989000	2.138632000
6	2.018160000	6.795173000	4.430564000
1	1.135202000	6.598106000	3.831660000
6	3.128496000	10.038668000	0.994258000
1	2.180731000	9.754301000	0.548785000
6	3.349467000	6.359043000	6.406555000
1	3.515231000	5.823156000	7.338711000
6	6.788251000	11.089077000	2.840543000
6	0.537797000	6.690655000	0.409699000
1	0.598629000	5.893108000	-0.331767000
6	2.218672000	6.114284000	5.621325000
1	1.480952000	5.378028000	5.941719000
6	0.380335000	8.738549000	2.316589000
1	0.341075000	9.531942000	3.063981000
6	5.139058000	11.386831000	0.959807000
1	5.764827000	12.145909000	0.495318000
6	5.863967000	7.000111000	7.977496000

1	5.055070000	7.141890000	8.708767000
1	6.782831000	7.451945000	8.366475000
1	6.023048000	5.916294000	7.866677000
6	-0.676663000	7.345242000	0.640908000
1	-1.565307000	7.057619000	0.077410000
6	3.917035000	11.002673000	0.391309000
1	3.575950000	11.467204000	-0.534128000
6	-0.755789000	8.366939000	1.593132000
1	-1.702801000	8.876751000	1.773907000
6	7.738526000	12.120143000	2.336011000
1	8.079174000	11.863453000	1.322066000
1	8.607253000	12.194669000	2.997300000
1	7.244561000	13.101421000	2.279270000
17	6.170224000	6.176430000	2.593302000
8	7.111845000	5.400097000	1.777528000
8	5.023704000	6.593731000	1.774214000
8	6.870968000	7.385489000	3.102254000
8	5.705769000	5.371371000	3.729169000

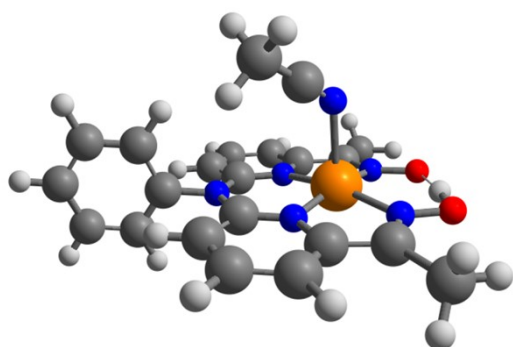
Table S11. 1 without solvent or perchlorate



29	5.509998000	9.175509000	4.398094000
8	8.001310000	10.637920000	4.765167000
8	7.369707000	8.989195000	6.571183000
7	2.808278000	8.411051000	2.785016000
1	7.814005000	9.958329000	5.580804000
7	4.756973000	9.800810000	2.721537000
7	4.079375000	7.935584000	4.760798000
7	6.244614000	8.533035000	6.086378000
7	6.929068000	10.446076000	3.972264000
6	3.603709000	9.393822000	2.172437000
6	5.508257000	7.616133000	6.674533000
6	4.288677000	7.266341000	5.938662000
6	1.594587000	8.063233000	2.062715000
6	3.005157000	7.709535000	3.990212000
6	1.636861000	7.042037000	1.113850000

1	2.574332000	6.517354000	0.926046000
6	5.542264000	10.754410000	2.134211000
6	2.049473000	6.746929000	4.398798000
1	1.172110000	6.543703000	3.793924000
6	3.180824000	9.968896000	0.945440000
1	2.250686000	9.659095000	0.480554000
6	3.375817000	6.314669000	6.379892000
1	3.537890000	5.780986000	7.313874000
6	6.781924000	11.104113000	2.858847000
6	0.469863000	6.712024000	0.420387000
1	0.490672000	5.915627000	-0.324141000
6	2.249750000	6.064322000	5.587965000
1	1.515486000	5.323020000	5.903925000
6	0.416819000	8.758976000	2.334679000
1	0.418118000	9.550889000	3.084472000
6	5.174023000	11.343808000	0.934598000
1	5.800710000	12.101719000	0.469622000
6	5.870953000	6.980917000	7.974411000
1	5.093310000	7.166637000	8.730351000
1	6.821584000	7.387604000	8.335212000
1	5.968156000	5.890626000	7.863084000
6	-0.718934000	7.401429000	0.681430000
1	-1.628253000	7.141421000	0.138223000
6	3.969979000	10.933177000	0.344931000
1	3.645954000	11.375618000	-0.597081000
6	-0.745850000	8.422681000	1.636954000
1	-1.672720000	8.959625000	1.840954000
6	7.746496000	12.115492000	2.343753000
1	8.108814000	11.825601000	1.346525000
1	8.599689000	12.210801000	3.022054000
1	7.256086000	13.095121000	2.243560000

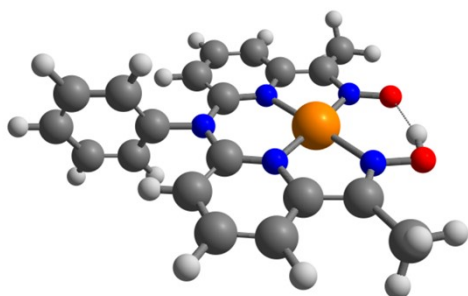
Table S12. 1 with bound acetonitrile



29	5.682608000	8.458134000	3.990993000
8	8.112755000	10.017005000	4.411833000
8	7.437264000	8.431360000	6.262670000
7	2.925702000	7.788467000	2.432593000
1	7.915046000	9.353797000	5.236253000
7	4.866169000	9.185692000	2.369522000
7	4.112966000	7.436405000	4.484411000
7	6.297453000	8.000078000	5.791235000
7	7.051029000	9.807206000	3.608840000
6	3.738704000	8.743423000	1.796677000
6	5.470796000	7.227985000	6.461613000
6	4.243076000	6.892519000	5.734390000
6	1.779217000	7.342566000	1.658794000
6	3.037131000	7.215645000	3.716524000
6	1.907347000	6.208826000	0.857128000
1	2.857387000	5.674936000	0.826724000
6	5.666138000	10.116985000	1.770740000
6	1.997816000	6.385073000	4.199763000
1	1.115417000	6.192340000	3.598630000
6	3.369144000	9.240415000	0.520521000
1	2.467147000	8.891089000	0.028856000
6	3.245069000	6.071837000	6.253102000
1	3.345001000	5.635599000	7.244623000
6	6.887331000	10.490338000	2.513440000
6	0.809385000	5.778146000	0.108125000
1	0.899186000	4.893027000	-0.522418000
6	2.118561000	5.824844000	5.462530000
1	1.318361000	5.186956000	5.838564000
6	0.580272000	8.052701000	1.729556000
1	0.511263000	8.935572000	2.366253000
6	5.340638000	10.646820000	0.529543000
1	5.979890000	11.386684000	0.052747000
6	5.744242000	6.736936000	7.843902000

1	4.971268000	7.086935000	8.544486000
1	6.720428000	7.100601000	8.181644000
1	5.742725000	5.637070000	7.874961000
6	-0.398361000	6.481002000	0.167954000
1	-1.253766000	6.142943000	-0.418155000
6	4.173834000	10.185216000	-0.093256000
1	3.890155000	10.569313000	-1.073143000
6	-0.512900000	7.616174000	0.977558000
1	-1.454684000	8.163671000	1.025037000
6	7.826357000	11.539173000	2.024961000
1	7.287565000	12.476686000	1.827275000
1	8.293188000	11.221230000	1.080373000
1	8.611755000	11.722416000	2.764468000
7	6.665032000	6.703155000	2.741574000
6	6.404222000	6.380130000	1.654603000
6	6.049587000	6.016716000	0.300178000
1	5.690284000	4.979267000	0.271253000
1	6.923089000	6.119215000	-0.357687000
1	5.250285000	6.683454000	-0.055689000

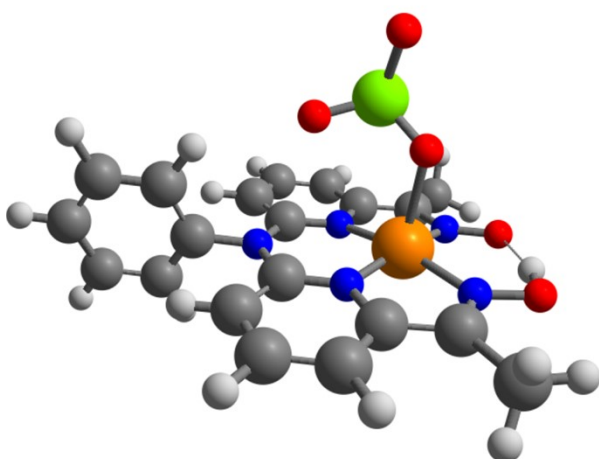
Table S13. Ligand oxidized **1-ox** without bound solvent or perchlorate



29	5.533429000	9.187214000	4.408935000
8	8.057685000	10.720596000	4.710518000
8	7.315890000	8.907284000	6.648829000
7	2.822471000	8.408526000	2.796578000
1	7.943179000	10.111024000	5.503540000
7	4.771262000	9.803698000	2.726256000
7	4.097011000	7.944841000	4.765622000
7	6.238655000	8.517290000	6.116572000
7	6.950663000	10.471697000	3.958648000
6	3.618597000	9.397800000	2.178953000
6	5.461814000	7.571067000	6.704089000
6	4.278085000	7.262468000	5.942035000
6	1.603200000	8.060267000	2.073567000
6	3.031041000	7.722579000	3.988826000

6	1.652580000	7.049159000	1.115282000
1	2.591847000	6.530867000	0.919650000
6	5.546496000	10.753896000	2.130938000
6	2.064213000	6.746288000	4.392363000
1	1.198295000	6.548015000	3.768616000
6	3.183318000	9.965216000	0.957447000
1	2.249590000	9.652328000	0.502230000
6	3.349018000	6.304515000	6.377249000
1	3.504176000	5.771734000	7.313232000
6	6.790309000	11.116367000	2.841929000
6	0.483464000	6.722555000	0.423955000
1	0.504230000	5.931619000	-0.326036000
6	2.233859000	6.053881000	5.578951000
1	1.493468000	5.313807000	5.879645000
6	0.427358000	8.752561000	2.359558000
1	0.429445000	9.537678000	3.116281000
6	5.169710000	11.339426000	0.927920000
1	5.794933000	12.095840000	0.458663000
6	5.821835000	6.941804000	7.993721000
1	5.037880000	7.131258000	8.742927000
1	6.773188000	7.341025000	8.357781000
1	5.904799000	5.850532000	7.878022000
6	-0.706413000	7.405618000	0.696022000
1	-1.616494000	7.146857000	0.153877000
6	3.966401000	10.930032000	0.345357000
1	3.635620000	11.369112000	-0.595386000
6	-0.735342000	8.417014000	1.661552000
1	-1.663894000	8.946622000	1.875578000
6	7.739087000	12.127529000	2.303890000
1	8.083881000	11.825798000	1.303898000
1	8.602938000	12.241465000	2.964219000
1	7.233824000	13.099134000	2.198806000

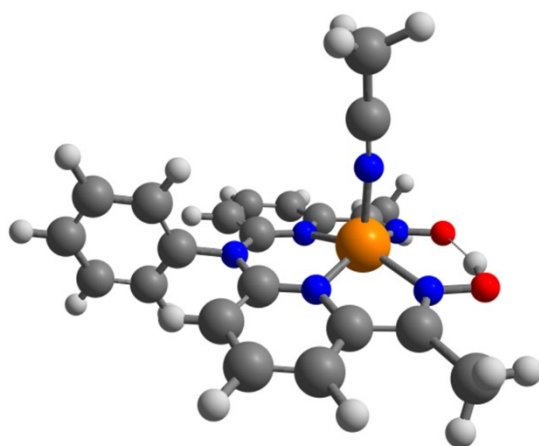
Table S14. Ligand oxidized **1-ox** with bound perchlorate



29	5.642202000	9.012935000	4.254940000
8	8.141605000	10.577985000	4.584207000
8	7.411345000	8.779696000	6.510223000
7	2.795514000	8.442578000	2.788533000
1	8.034680000	9.942635000	5.362822000
7	4.768072000	9.800204000	2.692978000
7	4.079981000	7.968817000	4.744623000
7	6.293281000	8.445119000	6.016616000
7	7.005639000	10.379886000	3.863137000
6	3.581696000	9.446597000	2.183881000
6	5.467024000	7.588546000	6.662337000
6	4.260022000	7.302603000	5.926321000
6	1.593555000	8.076019000	2.048662000
6	3.010730000	7.747434000	3.973775000
6	1.690836000	7.111983000	1.046478000
1	2.652883000	6.644466000	0.837000000
6	5.526576000	10.775797000	2.119981000
6	2.052450000	6.763683000	4.372803000
1	1.201241000	6.541502000	3.737095000
6	3.097721000	10.088664000	1.019296000
1	2.134538000	9.820233000	0.598206000
6	3.319843000	6.362285000	6.377890000
1	3.465602000	5.845839000	7.324095000
6	6.801282000	11.091300000	2.795500000
6	0.539988000	6.766633000	0.334139000
1	0.598439000	6.011570000	-0.450178000
6	2.216480000	6.089604000	5.570533000
1	1.482018000	5.344107000	5.872492000
6	0.387086000	8.703566000	2.357007000
1	0.352500000	9.455034000	3.146429000
6	5.102318000	11.434430000	0.969841000

1	5.715968000	12.210024000	0.516889000
6	5.822117000	6.997288000	7.972819000
1	4.944657000	6.917005000	8.625593000
1	6.594039000	7.602768000	8.459825000
1	6.226666000	5.981818000	7.825379000
6	-0.679903000	7.384551000	0.628479000
1	-1.575399000	7.111466000	0.069257000
6	3.867912000	11.074178000	0.422899000
1	3.499691000	11.571172000	-0.474137000
6	-0.756978000	8.349818000	1.637649000
1	-1.708277000	8.830016000	1.867924000
6	7.728029000	12.136308000	2.281925000
1	8.034956000	11.895692000	1.253505000
1	8.616987000	12.212163000	2.914043000
1	7.220278000	13.111719000	2.254987000
17	6.172854000	6.080410000	2.837030000
8	7.091856000	5.278542000	2.031698000
8	4.916232000	6.303024000	2.113027000
8	6.822860000	7.404945000	3.096636000
8	5.903010000	5.424143000	4.119512000

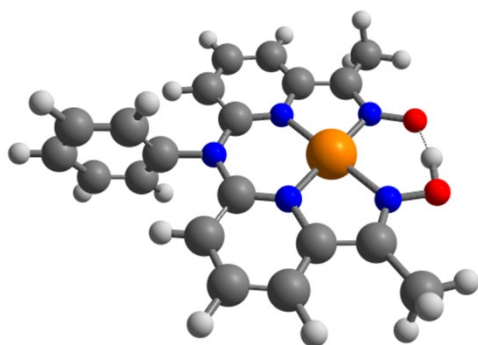
Table S15. Ligand oxidized **1-ox** with bound acetonitrile



29	5.737270000	8.268227000	3.700194000
8	8.211837000	9.876705000	4.092022000
8	7.468408000	8.116464000	6.004433000
7	2.776550000	7.924010000	2.376563000
1	8.109205000	9.219408000	4.857505000
7	4.763485000	9.254647000	2.285798000
7	4.062872000	7.445060000	4.327858000
7	6.331338000	7.824030000	5.527458000
7	7.051296000	9.730799000	3.401575000

6	3.559573000	8.943362000	1.789930000
6	5.432247000	7.131841000	6.263330000
6	4.195331000	6.878122000	5.564582000
6	1.584367000	7.549847000	1.624486000
6	2.955369000	7.279103000	3.598005000
6	1.694186000	6.549241000	0.660592000
1	2.655059000	6.063216000	0.489554000
6	5.505945000	10.264636000	1.756810000
6	1.918263000	6.419290000	4.077079000
1	1.037576000	6.232615000	3.470655000
6	3.053242000	9.641508000	0.669177000
1	2.082362000	9.393775000	0.252442000
6	3.174579000	6.073146000	6.100879000
1	3.277001000	5.630760000	7.088770000
6	6.801316000	10.532330000	2.409135000
6	0.556473000	6.190908000	-0.067293000
1	0.625162000	5.407521000	-0.822411000
6	2.040640000	5.833473000	5.325124000
1	1.245707000	5.188156000	5.696707000
6	0.377788000	8.201671000	1.880532000
1	0.331903000	8.981396000	2.641575000
6	5.051779000	10.996204000	0.660649000
1	5.654262000	11.800371000	0.243849000
6	5.760451000	6.716004000	7.646004000
1	4.911766000	6.256987000	8.158479000
1	6.099539000	7.591574000	8.219728000
1	6.602701000	6.005652000	7.629294000
6	-0.662206000	6.832117000	0.174951000
1	-1.547361000	6.548700000	-0.395403000
6	3.810241000	10.662741000	0.115059000
1	3.424149000	11.207583000	-0.745919000
6	-0.752136000	7.834256000	1.146829000
1	-1.703099000	8.332321000	1.336913000
6	7.700546000	11.630159000	1.959524000
1	7.171127000	12.593241000	1.997840000
1	8.006538000	11.463310000	0.916030000
1	8.592380000	11.684049000	2.589727000
7	6.523114000	6.729731000	2.562797000
6	6.872036000	5.861326000	1.880098000
6	7.310481000	4.777843000	1.031658000
1	6.885449000	3.831597000	1.393781000
1	8.407266000	4.715330000	1.050906000
1	6.974201000	4.957407000	0.001212000

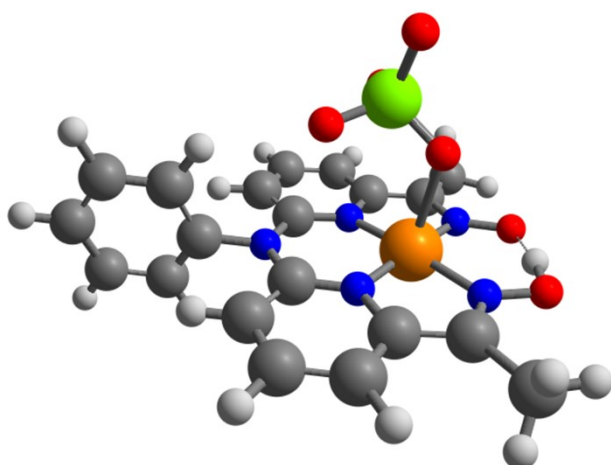
Table S16. Metal oxidized **1** without bound perchlorate or solvent



29	5.494580000	9.172240000	4.381679000
8	7.961697000	10.566366000	4.755895000
8	7.341453000	9.007552000	6.501829000
7	2.795150000	8.419307000	2.785757000
1	7.798841000	9.894674000	5.603850000
7	4.750366000	9.793707000	2.750560000
7	4.094758000	7.963126000	4.745791000
7	6.235800000	8.550144000	6.044090000
7	6.909198000	10.402499000	3.981065000
6	3.592999000	9.395700000	2.196564000
6	5.505512000	7.634847000	6.642818000
6	4.295025000	7.287738000	5.926121000
6	1.583785000	8.060821000	2.056657000
6	3.011968000	7.735882000	3.979598000
6	1.646176000	7.040500000	1.108687000
1	2.589898000	6.525647000	0.925735000
6	5.536747000	10.750042000	2.156518000
6	2.062403000	6.772986000	4.404491000
1	1.186469000	6.580747000	3.793504000
6	3.175704000	9.986168000	0.975498000
1	2.240369000	9.674478000	0.521906000
6	3.386496000	6.343840000	6.373654000
1	3.558531000	5.818143000	7.310112000
6	6.764933000	11.074318000	2.868936000
6	0.484935000	6.700739000	0.410995000
1	0.516488000	5.905174000	-0.333696000
6	2.255547000	6.091076000	5.588708000
1	1.520009000	5.353317000	5.907997000
6	0.401488000	8.748060000	2.327958000
1	0.392700000	9.539276000	3.078230000
6	5.166425000	11.346823000	0.965408000
1	5.802316000	12.102318000	0.509438000

6	5.896918000	7.020333000	7.940058000
1	5.123964000	7.222686000	8.696375000
1	6.853858000	7.418261000	8.287970000
1	5.976510000	5.929151000	7.827012000
6	-0.710935000	7.379075000	0.668311000
1	-1.615161000	7.110478000	0.121101000
6	3.959039000	10.949705000	0.375270000
1	3.632608000	11.399857000	-0.561730000
6	-0.753488000	8.399611000	1.623998000
1	-1.686480000	8.926952000	1.823760000
6	7.751673000	12.070320000	2.376634000
1	8.102978000	11.779880000	1.375487000
1	8.606133000	12.145868000	3.053670000
1	7.270216000	13.055473000	2.286832000

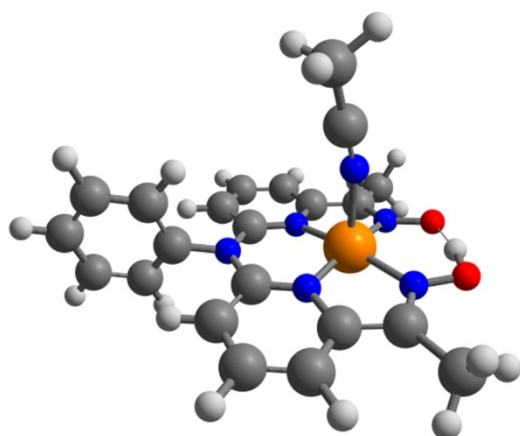
Table S17. Metal oxidized **1** with perchlorate



29	5.526490000	9.108531000	4.325423000
8	8.008050000	10.487483000	4.684215000
8	7.404796000	8.900164000	6.414604000
7	2.756772000	8.463236000	2.808863000
1	7.849648000	9.805028000	5.523976000
7	4.729257000	9.810521000	2.751534000
7	4.066176000	7.993593000	4.757991000
7	6.262478000	8.497927000	5.994866000
7	6.927620000	10.364030000	3.939613000
6	3.557760000	9.433539000	2.215060000
6	5.508396000	7.621314000	6.620144000
6	4.272767000	7.311539000	5.931264000
6	1.567190000	8.076667000	2.061155000
6	2.978937000	7.773308000	3.997788000

6	1.672936000	7.055555000	1.117612000
1	2.633071000	6.564031000	0.959531000
6	5.515219000	10.765687000	2.157826000
6	2.026921000	6.816010000	4.426543000
1	1.144710000	6.631966000	3.822259000
6	3.125450000	10.045193000	1.010289000
1	2.175051000	9.755887000	0.573549000
6	3.358088000	6.377259000	6.388108000
1	3.537268000	5.844131000	7.318832000
6	6.763261000	11.062392000	2.847809000
6	0.534323000	6.686450000	0.397845000
1	0.599868000	5.889924000	-0.343740000
6	2.222350000	6.131866000	5.609906000
1	1.485004000	5.396782000	5.931282000
6	0.363165000	8.735167000	2.306863000
1	0.320324000	9.528099000	3.054171000
6	5.132002000	11.381799000	0.979661000
1	5.770645000	12.133025000	0.520694000
6	5.911772000	6.993761000	7.907814000
1	5.098757000	7.085206000	8.641491000
1	6.814688000	7.465720000	8.304787000
1	6.105306000	5.921148000	7.753386000
6	-0.682627000	7.336304000	0.628797000
1	-1.568982000	7.045013000	0.064111000
6	3.910515000	11.005835000	0.406484000
1	3.572602000	11.471230000	-0.518953000
6	-0.768973000	8.357495000	1.580939000
1	-1.718322000	8.862584000	1.760421000
6	7.749724000	12.057257000	2.350809000
1	8.092091000	11.768828000	1.345877000
1	8.610537000	12.125217000	3.020696000
1	7.272919000	13.045007000	2.268713000
17	6.187016000	6.234544000	2.690287000
8	7.156187000	5.476870000	1.899638000
8	5.034016000	6.610229000	1.861315000
8	6.852397000	7.479374000	3.180184000
8	5.739084000	5.449072000	3.844266000

Table S18. Metal oxidized **1** with acetonitrile



29	5.574144000	8.526575000	3.874436000
8	8.100207000	9.837942000	4.194987000
8	7.465419000	8.275139000	5.949777000
7	2.772502000	7.966865000	2.410083000
1	7.937592000	9.169301000	5.037841000
7	4.735409000	9.325695000	2.363807000
7	4.046282000	7.531052000	4.390619000
7	6.288091000	7.951308000	5.563836000
7	6.980269000	9.784632000	3.499600000
6	3.557185000	8.965273000	1.833816000
6	5.476413000	7.189660000	6.265094000
6	4.213670000	6.916043000	5.608044000
6	1.619739000	7.535423000	1.629924000
6	2.945684000	7.338603000	3.643522000
6	1.787460000	6.488600000	0.724415000
1	2.763954000	6.015003000	0.618652000
6	5.508333000	10.308283000	1.799488000
6	1.935499000	6.470035000	4.123823000
1	1.041844000	6.307027000	3.530068000
6	3.105995000	9.613109000	0.656467000
1	2.152050000	9.333216000	0.220660000
6	3.239045000	6.069760000	6.114625000
1	3.377529000	5.579116000	7.074687000
6	6.779463000	10.559639000	2.467349000
6	0.689680000	6.069816000	-0.031165000
1	0.805446000	5.252764000	-0.743689000
6	2.089711000	5.850118000	5.348200000
1	1.307618000	5.185494000	5.714175000
6	0.391358000	8.173227000	1.801989000
1	0.297196000	8.989813000	2.518732000
6	5.101165000	10.970170000	0.653893000

1	5.726774000	11.742482000	0.212481000
6	5.900931000	6.670807000	7.593479000
1	5.068915000	6.196596000	8.121207000
1	6.294121000	7.495032000	8.204888000
1	6.710796000	5.935649000	7.466963000
6	-0.549936000	6.697490000	0.127513000
1	-1.404580000	6.367935000	-0.464271000
6	3.875932000	10.604811000	0.081886000
1	3.522385000	11.103062000	-0.820269000
6	-0.699398000	7.746130000	1.041445000
1	-1.666395000	8.234496000	1.163700000
6	7.764175000	11.570810000	2.000855000
1	7.253962000	12.511954000	1.758028000
1	8.256657000	11.208857000	1.084656000
1	8.526159000	11.753372000	2.763962000
7	6.459641000	6.818161000	2.638921000
6	6.668746000	5.974869000	1.870653000
6	6.928985000	4.924205000	0.912154000
1	6.185014000	4.124717000	1.031381000
1	7.934521000	4.512763000	1.076160000
1	6.866217000	5.330875000	-0.106475000

References

1. A. Das, A. Ali, G. Gupta, A. Santra, P. Jain, P. P. Ingole, S. Paul and S. Paria, *ACS Catal.*, 2023, **13**, 5285-5297.
2. C. E. Paul, S. Gargiulo, D. J. Opperman, I. Lavandera, V. Gotor-Fernandez, V. Gotor, A. Taglieber, I. W. C. E. Arends and F. Hollmann, *Org. Lett.*, 2013, **15**, 180-183.
3. W. C. Wolsey, *J. Chem. Educ.*, 1973, **50**, A335-A337.
4. (a) S. K. Sur, *J. Magn. Reson.*, 1989, **82**, 169-173; (b) G. A. Bain and J. F. Berry, *J. Chem. Educ.*, 2008, **85**, 532-536.
5. E. P. Parry and R. A. Osteryoung, *Anal. Chem.*, 1965, **37**, 1634-1637.
6. APEX II 2009 Ed.; Bruker Analytical X-ray Systems Inc.: Madison, WI, 2009
7. G. M. Sheldrick, *Acta Crystallogr., Sect. A Found. Crystallogr.*, 2008, **A64**, 112-122.
8. C. F. Macrae, I. J. Bruno, J. A. Chisholm, P. R. Edgington, P. McCabe, E. Pidcock, L. Rodriguez-Monge, R. Taylor, J. van de Streek and P. A. Wood, *J. Appl. Crystallogr.*, 2008, **41**, 466-470.
9. B. Ravel and M. Newville, *J. Synchrotron Radiat.*, 2005, **12**, 537-541.
10. J. J. Rehr and R. C. Albers, *Rev. Mod. Phys.*, 2000, **72**, 621-654.
11. D. C. Koningsberger, R. Prins and Editors, *X-ray Absorption: Principles, Applications, Techniques of EXAFS SEXAFS, and XANES*, 1988.
12. F. Neese, *Wiley Interdiscip. Rev. Comput. Mol. Sci.*, 2012, **2**, 73-78.
13. A. D. Becke, *Phys. Rev. A Gen. Phys.*, 1988, **38**, 3098-3100.
14. F. Weigend and R. Ahlrichs, *Phys. Chem. Chem. Phys.*, 2005, **7**, 3297-3305.

15. (a) S. Grimme, J. Antony, S. Ehrlich and H. Krieg, *J. Chem. Phys.*, 2010, **132**, 154104/154101-154104/154119; (b) S. Grimme, S. Ehrlich and L. Goerigk, *J. Comput. Chem.*, 2011, **32**, 1456-1465.
16. S. Kossmann and F. Neese, *J. Chem. Theory Comput.*, 2010, **6**, 2325-2338.
17. (a) A. D. Becke, *J. Chem. Phys.*, 1993, **98**, 5648-5652; (b) P. J. Stephens, F. J. Devlin, C. F. Chabalowski and M. J. Frisch, *J. Phys. Chem.*, 1994, **98**, 11623-11627.
18. X. Sui, A. C. Weitz, E. R. Farquhar, M. Badiee, S. Banerjee, J. von Lintig, G. P. Tochtrop, K. Palczewski, M. P. Hendrich and P. D. Kiser, *Biochemistry*, 2017, **56**, 2836-2852.
19. B. Bossmann, L. H. Grimme and J. Knoetzel, *Planta*, 1999, **207**, 551-558.
20. D. Yang, K. Yan, W. Wei, L. Tian, Q. Li, J. You and H. Wang, *RSC Adv.*, 2014, **4**, 48547-48553.